Investigation of dislocation dynamics by nuclear magnetic resonance

D. Wolf* and O. Kanert†
Department of Physics, University of Utah, Salt Lake City, Utah 84112
(Received 11 April 1977)

Inspired by recent experiments of Sleeswyk, Kanert *et al.* investigating the effect of plastic deformation on the simultaneously measured nuclear spin-lattice relaxation time $T_{1\rho}$ in the rotating frame, the influence of moving dislocations on $T_{1\rho}$ is studied theoretically. As illustrated recently by Wolf, this necessitates the calculation of quadrupolar "lattice" correlation functions associated with the relative motion of dislocations and nuclear spins. Assuming discrete and random dislocation jumps during (i) plastic deformation, (ii) internal friction, and (iii) fatique experiments, these correlation functions are determined. Their general form allows prediction of $T_{1\rho}$ in both the strong-collision (Rowland-Fradin) and the quadrupolar weak-collision region. It is demonstrated how, from low-field $T_{1\rho}$ experiments performed during either one of the three types of deformation modes, dislocation parameters such as the mobile and immobile dislocation density, the mean time between successive jumps of a dislocation, and the distribution of loop lengths and jump widths may be extracted. As a declared goal, this article aims at the understanding of the properties of the $T_{1\rho}$ minimum (i.e., of its position, depth, and width) in terms of the underlying microscopic mechanism of dislocation motion, an information which, in the past, could not be gained from purely mechanical (e.g., internal friction) experiments. Consequently, a variety of new combined NMR-deformation experiments is proposed to investigate the microscopic dynamics of dislocation motion.

I. INTRODUCTION

One of the most interesting new applications of nuclear-magnetic-resonance (NMR) techniques in solid-state physics and materials science investigates the effect of plastic deformation on the spin-lattice relaxation time in the rotating frame, $T_{1\rho}$. In a series of articles by Hut *et al.*[1-4] and Hackelöer *et al.*,[5] $T_{1\rho}$ has been studied as a function of the plastic-deformation rate $\dot{\epsilon}$ which was varied over a fairly wide range ($10^{-4} \lesssim \dot{\epsilon} \lesssim 10^{2}$). These first experiments performed on NaCl, NaF, and RbCl single crystals (via the resonance of the ^{23}Na and ^{87}Rb spins, respectively), clearly exhibit the following four effects:

(i) The total relaxation rate $T_{1\rho}^{-1}$ in a weak rotating field may be decomposed into a static background contribution $(T_{1\rho}^{-1})_s$ and the contribution $(T_{1\rho}^{-1})_{\rm def}$ which is governed by the deformation rate $\dot{\epsilon}$:

$$1/T_{1\rho} = (1/T_{1\rho})_s + (1/T_{1\rho})_{\rm def} \,. \tag{1.1}$$

(ii) In the limited range in which $10^{-4} < \dot{\epsilon} < 1$ sec^{-1} $(T_{1\rho}^{-1})_{\rm def}$ is found to be proportional to $\dot{\epsilon}$, but independent of the actual deformation ϵ of the crystal.[1-4] For larger values of $\dot{\epsilon}$ a maximum of $(T_{1\rho}^{-1})_{\rm def}$, which appears whenever $\dot{\epsilon}$ is about equal to 20 sec^{-1}, is observed.[5]

(iii) The comparison of the $(T_{1\rho})_{\rm def}$ values obtained for the ^{23}Na resonance in NaCl with those measured from the ^{87}Rb resonance in RbCl, clearly shows that $(T_{1\rho})_{\rm def}$ is governed by fluctuating *quadrupolar* interactions while dipolar interactions seem to play a minor role only. This observation was also confirmed by the absence of plastic-deformation effects on the ^{19}F resonance in KF, a nucleus well known for its lack of an electric quadrupole moment ($I = \frac{1}{2}$).

(iv) Between +20 and −60 °C $(T_{1\rho})_{\rm def}$ is practically independent of temperature.

From these experimental results Hut *et al.* concluded that the microscopic processes causing the observed phenomena are closely related to the long-range migration of dislocations during plastic deformation.

In spite of some advantages over purely mechanical methods to investigate dislocation dynamics, two types of difficulties are inherent to this new technique.

First, *experimentally* it is difficult to obtain accurate values of $(T_{1\rho}^{-1})_{\rm def}$ during the rather short time interval during which the crystal may be deformed without breaking. The same problem makes it very difficult to investigate the exponentiality of the relaxation decay of the spin-locked magnetization. Also, as illustrated in the latest article by Kanert *et al.*,[5] as a practical limit $\dot{\epsilon}$ may not exceed a value of about 10^{2} sec^{-1} for the crystals not to break during the spin-locking $T_{1\rho}$ experiment. Since the shortest values of $(T_{1\rho})_{\rm def}$ are observed for $10^{1} \lesssim \dot{\epsilon} \lesssim 10^{2}$ sec^{-1}, the *entire* $(T_{1\rho})_{\rm def}$ minimum, which contains a considerable amount of information on the microscopic mechanisms of dislocation motion[5] (see below), cannot be observed if the dis-

location jumps are being induced by the plastic deformation of the sample.

Secondly, the *theoretical interpretation* of the measured $(T_{1\rho})_{def}$ values, for example, in terms of the mean time τ_d between successive jumps of a dislocation and the density ρ_m of mobile dislocations is not unambiguous. The main reason, therefore, lies in the increase of the plastic deformation ϵ *during* the NMR experiment which results in increases of both ρ_m and the quadrupolar contribution H_Q to the local field experienced by the nuclear spins. Another problem arises from point defects (vacancies, interstitials) produced by nonconservative movements of dislocations during plastic deformation. The NMR relaxation contribution of such defects is fairly unknown and may thus complicate the interpretation of these experiments.

Some of the experimental difficulties outlined above may be overcome by deforming the crystal periodically (for example, sinusoidally) instead of applying a constant time-independent stress. In practice, this would mean to investigate dislocation dynamics during internal-friction or fatigue experiments and not during plastic deformation. During such experiments enough time is available to measure $(T_{1\rho})_{def}$ fairly accurately. Also, larger values of $\dot{\epsilon}$ ($>10^2$ sec^{-1}) may thus be obtained. This should enable the investigation of the *entire* minimum of $(T_{1\rho})_{def}$ and not only its "slow motion" side as in the plastic-deformation experiments by Hut *et al*.

While internal-friction experiments permit investigation of the stringlike vibration of dislocations, in that they provide also information on the long-range migration of dislocations (unpinning) fatigue–NMR experiments are more similar to the plastic-deformation–NMR experiments of Hut *et al*. The systematic investigation of both should, therefore, allow separation of the NMR relaxation effects associated with the *dislocation motion* from those arising from the *point defects* created during plastic-deformation and fatigue experiments. Also, some of the difficulties encountered in the theoretical interpretation of $(T_{1\rho})_{def}$ values (see above) may thus be overcome.

To analyze what type of information on the mechanisms of dislocation motion may be extracted from the experiments proposed above, in this article the NMR relaxation behavior is investigated for an *arbitrary* method used to deform the crystal (Secs. II and III). In particular, in Secs. IV–VI the expected effects of plastic-deformation, internal-friction, and fatigue experiments, respectively, on $T_{1\rho}$ are discussed. As illustrated there, these types of experiments are expected to yield a considerable amount of information on the microscopic mechanisms of dislocation motion.

II. ROTATING-FRAME QUADRUPOLAR SPIN-LATTICE RELAXATION ASSOCIATED WITH THE MOTION OF LATTICE DEFECTS IN CUBIC CRYSTALS

A. General theory

In cubic crystals electric field gradients (EFG's) at the nuclear-spin positions are usually due to structural defects, such as vacancies, interstitial atoms, dislocations, etc.[6] Whenever, for example, a dislocation changes its position in the crystal, the surrounding atoms have to move also thus (for $I \geq 1$) causing fluctuations of both the quadrupolar and the dipolar spin Hamiltonian. As verified by Hut *et al*[1-4] and Hackelöer *et al*.,[5] however, the *dipolar* effects on the nuclear-spin relaxation due to dislocation motion are negligible, and *quadrupolar* effects dominate the observed relaxation behavior. Therefore, in what follows we shall concentrate exclusively on the effect of quadrupolar fluctuations due to the motion of lattice defects on the nuclear-spin relaxation.

For the investigation of rather infrequent atomic or defect motions, the spin-lattice relaxation time $T_{1\rho}$ in a weak rotating field H_1 has proved to be the most appropriate NMR parameter affected by such motions. In reviewing the basic expressions for $(T_{1\rho})_Q^{-1}$ due to fluctuations of quadrupolar interactions, we limit ourselves to the simple case in which (i) all N spins of the sample are identical and (ii) the rotating field is applied at the exact resonance-precession frequency $\omega = \omega_0 = \gamma H_0$ of these spins.

From a thermodynamic point of view, the entire Hamiltonian of a spin system imbedded in a crystal may be decomposed into the Hamiltonians $\mathcal{H}_S$ and $\mathcal{H}_L$ of the spin system and the "lattice" and their interaction Hamiltonian $\mathcal{H}_{SL}$:

$$\mathcal{H} = \mathcal{H}_S + \mathcal{H}_{SL} + \mathcal{H}_L . \tag{2.1}$$

Neglecting all *explicitly* time-dependent (nonsecular) interactions in the rotating frame,[7] the Hamiltonian $\mathcal{H}_S$ of the isolated spin system imbedded in the crystal reads as follows[8]:

$$\mathcal{H}_S = \mathcal{H}_Z^r + \mathcal{H}_D^{(0)RL} + \mathcal{H}_Q^{(0)RL} , \tag{2.2}$$

where $\mathcal{H}_D^{(0)RL}$ and $\mathcal{H}_Q^{(0)RL}$ represent the secular parts of the rigid-lattice dipolar and quadrupolar Hamiltonians, respectively, in the *laboratory* frame, i.e., $\mathcal{H}_D^{(0)RL}$ and $\mathcal{H}_Q^{(0)RL}$ commute with the laboratory-frame Zeeman Hamiltonian $\mathcal{H}_Z$. The Zeeman Hamiltonian $\mathcal{H}_Z^r$ in the rotating frame is given by[7] (at exact resonance)

$$\mathcal{H}_Z^r = -\gamma\hbar H_1 \sum_{j=1}^{N} I_{jx}^r , \tag{2.3}$$

where I^r_{jx} denotes the x component of the angular momentum operator $\vec{I}^r_j$ of spin j referred to the rotating reference frame. Both $\mathcal{H}_D^{(0)}$ and $\mathcal{H}_Q^{(0)}$ may generally be decomposed into spin-operator terms and lattice functions, according to[9]

$$\mathcal{H}_D^{(0)} = \frac{1}{2}\sum_{i=1}^{N}\sum_{j=1}^{N} A_{ij}^{(0)} F_{ij}^{(0)}, \tag{2.4}$$

$$\mathcal{H}_Q^{(0)} = \sum_{m=1}^{N}\sum_{\nu=1}^{\nu_{\max}}\sum_{k_\nu=1}^{N_d^\nu} Q_n^{(0)} V_{k_\nu n}^{(0)}, \tag{2.5}$$

where the dipolar spin operators $A_{ij}^{(0)}$ and the lattice functions $F_{ij}^{(0)}$ are governed by the usual expressions.[8,9] In the quadrupolar Hamiltonian (2.5) for a *cubic* crystal, a sum over $\nu_{\max}$ different types of structural defects, which eventually distort the crystal lattice, has been performed. N_d^ν denotes the number of defects of the particular type ν. Then $V_{k_\nu j}^{(0)}$ represents the EFG at the site of spin j which is due to a defect k_ν of type ν, and[10]

$$V_{k_\nu j}^{(0)} = eq_{k_\nu j}(3\cos^2\theta_{k_\nu j} - 1 + \eta_{k_\nu j}\sin^2\theta_{k_\nu j}\cos 2\phi_{k_\nu j}). \tag{2.6}$$

Here $eq_{k_\nu j}$ and $\eta_{k_\nu j}$ denote the *magnitude* and *asymmetry parameter* of the EFG at the position of spin j which is produced by some defect k_ν. $\theta_{k_\nu j}$ and $\phi_{k_\nu j}$ characterize the orientation of the symmetry axis of the EFG tensor associated with defect k_ν with respect to the "magnetic" coordinate system (with its z axis parallel to H_0).[6,8] The quadrupolar spin-operator terms are given by

$$Q_n^{(0)} = [eQ/4I(2I-1)][I_{nz}^2 - \tfrac{1}{4}(I_n^+ I_n^- + I_n^- I_n^+)] = -[eQ/8I(2I-1)](3I_{nz}^2 - \vec{I}^2). \tag{2.7}$$

If "lattice"-induced fluctuations of both the dipolar and the quadrupolar reservoir may be activated, the spin-lattice interaction Hamiltonian in Eq. (2.1) reads as follows[8,11]:

$$\mathcal{H}_{SL} = \mathcal{H}_D^{(0)} - \mathcal{H}_D^{(0)\mathrm{RL}} + (\mathcal{H}_Q^{(0)})_{\mathrm{dyn}} - (\mathcal{H}_Q^{(0)\mathrm{RL}})_{\mathrm{dyn}}, \tag{2.8}$$

where $(\mathcal{H}_Q^{(0)})_{\mathrm{dyn}}$ represents that part of the secular quadrupole Hamiltonian that actually fluctuates. This definition takes into account that not all types of structural defects are necessarily mobile. As an example, one may think of mobile ($\nu=1$) and immobile ($\nu=2$) dislocations or point defects which produce the EFG's in the quadrupolar Hamiltonian (2.5).

By their very definition, $\mathcal{H}_D^{(0)\mathrm{RL}}$ and $\mathcal{H}_Q^{(0)\mathrm{RL}}$ are part of the *isolated* spin system, i.e., they commute with $\mathcal{H}_L$ in Eq. (2.1). The lattice-induced time dependence of $\mathcal{H}_{SL}$ is, therefore, governed by the following expression[8,11]:

$$\mathcal{H}_{SL}(t) = e^{(i/\hbar)\mathcal{H}_L t}\mathcal{H}_{SL}e^{-(i/\hbar)\mathcal{H}_L t} = \mathcal{H}_D^{(0)}(t) - \mathcal{H}_D^{(0)\mathrm{RL}} + [\mathcal{H}_Q^{(0)}(t)]_{\mathrm{dyn}} - [\mathcal{H}_Q^{(0)\mathrm{RL}}]_{\mathrm{dyn}}. \tag{2.9}$$

Considering $\mathcal{H}_{SL}(t)$ as a perturbation on the isolated spin system characterized by $\mathcal{H}_S$, the relaxation behavior of the nuclear-spin system under the effect of lattice-induced dipolar and quadrupolar fluctuations may be determined. If the average quadrupolar local field $H_{Q\rho}$ experienced by the nuclear spins is not considerably larger than the dipolar local field $H_{D\rho}$ ($H_{Q\rho} \approx H_{D\rho}$), a *single spin temperature* may be assigned to the isolated spin reservoir.[11,12] As illustrated by Wolf,[8] the Bloch-Wangsness-Redfield or Hebel-Slichter theory may then be applied to verify that the entire spin-lattice relaxation rate $T_{1\rho}^{-1}$ may be decomposed into a dipolar and a quadrupolar contribution, according to

$$1/T_{1\rho} = (1/T_{1\rho})_D + (1/T_{1\rho})_Q. \tag{2.10}$$

It has been demonstrated experimentally[1-5] that for the motion of dislocations during plastic deformation the dipolar relaxation contribution in Eq. (2.10) is negligible if the temperature is low enough to avoid self-diffusion. (The deeper theoretical reasons therefore are discussed in some detail in Sec. III B.) In what follows we shall, therefore, restrict our analysis to the quadrupolar relaxation contribution.

If we start from the original papers[8,13] and use a more general formalism, we may derive the following expression for $(T_{1\rho})_Q$ (at exact resonance)[11]:

$$\left(\frac{1}{T_{1\rho}}\right)_Q = \frac{\delta_Q}{4\omega_{\mathrm{eff}}^2}\sum_{q=0}^{2} h^{(q)}\left(-\left.\frac{dG_Q^{(0)}(t)}{dt}\right|_{t=0} - \mathrm{Re}\int_0^\infty dt\ \frac{d^2G_Q^{(0)}(t)}{dt^2}\ k_Q(t)e^{iq\Omega t}\right), \tag{2.11}$$

where δ_Q was defined as follows:

$$\delta_Q = \tfrac{3}{80}\,[e^2Q^2(2I+1)/I^2(2I-1)\hbar^2]. \tag{2.12}$$

The classical quadrupolar "lattice" correlation function $G_Q^{(0)}(t)$ is given by

$$G_Q^{(0)}(t) = \frac{1}{N}\sum_{j=1}^{N}\sum_{k=1}^{N_d^{\mathrm{dyn}}} \langle V_{kj}^{(0)}(t'+t)V_{kj}^{(0)*}(t')\rangle_{t'}, \tag{2.13}$$

where N_d^{dyn} denotes the number of *mobile* defects which, for simplicity, were assumed to be all of the same type (e.g., $\nu=1$). The angular brackets symbolize a time average over the initial time t'.

The "quadrupolar spin-correlation function" $k_Q(t)$ describes the thermal mixing, following a dislocation jump, of the secular part of $\mathcal{H}_Q^{(0)}$ in the *rotating* frame with $\mathcal{H}_Z^r$ and with the secular part

of $\mathcal{H}_D^{(0)}$ with respect to $\mathcal{H}_Z^r$. At $t=0$, $k_Q(t)$ equals unity while for times that are much longer than the "quadrupolar-thermal-mixing time" T_{mQ}, $k_Q(t)$ must vanish,[8,11] i.e.,

$$k_Q(0)=1\,;\quad k_Q(t\to\infty)=0\,. \tag{2.14}$$

The "effective precession frequency" ω_{eff} in Eq. (2.11), defined by[11]

$$\omega_{eff}^2=\omega_1^2+\omega_{Dr}^2+(\omega_{Qr}^{(n)})^2+[1-k_Q(\tau_{cQ})]^2(\omega_{Qr}^{(0)})^2\,, \tag{2.15}$$

is proportional to the effective heat capacity of the spin system, i.e., to the heat capacity of that part of the spin system which is able to maintain a common spin temperature even during the quadrupolar fluctuations. Here, τ_{cQ} denotes the quadrupolar pair correlation time, i.e., the mean time between successive relative jumps of a spin-defect pair. [Note that $1-k_Q(\tau_{cQ})$ denotes the probability that on the average, between successive relative jumps of a spin-defect pair, quadrupolar thermal mixing may take place.]

With respect to the Zeeman Hamiltonian (2.3) in the *rotating* frame, $\mathcal{H}_D^{(0)}$ and $\mathcal{H}_Q^{(0)}$ contain secular and nonsecular contributions.[11] The corresponding local-field precession frequencies which appear in Eq. (2.15) are given by[10,11]

$$(\omega_{Dr}^{(0)})^2=\tfrac{1}{3}(\omega_{Dr}^{(n)})^2=\tfrac{1}{4}\omega_{Dr}^2$$
$$=\frac{\delta_D}{16}\frac{1}{N}\sum_i\sum_j|F_{ij}^{(0)\mathrm{RL}}|^2\,, \tag{2.16}$$

$$(\omega_{Qr}^{(0)})^2=\tfrac{1}{3}\omega_{Qr}^{(n)2}=\tfrac{1}{4}\omega_{Qr}^2$$
$$=\frac{\delta_Q}{16}\frac{1}{N}\sum_{n=1}^{N}\sum_{\nu=1}^{\nu_{\max}}\sum_{k_\nu=1}^{N_d^\nu}|V_{k_\nu n}^{(0)}|^2\,, \tag{2.17}$$

where analogous to Eq. (2.12), δ_D is given by

$$\delta_D=\gamma^4\hbar^2I(I+1)\,. \tag{2.18}$$

In terms of the above local-field precession frequencies, the frequency Ω in Eq. (2.11) may be written as follows[11]:

$$\Omega^2=\omega_{eff}^2+2\omega_{Dr}^{(0)}(\omega_{Dr}^{(n)}+\omega_{Qr}^{(n)})+2\omega_{Dr}^{(n)}\omega_{Qr}^{(n)}$$
$$+2\omega_{Qr}^{(0)}[1-k_Q(\tau_{cQ})]^2(\omega_{Qr}^{(n)}+\omega_{Dr}^{(n)})\,. \tag{2.19}$$

In writing this expression it was observed that $\mathcal{H}_Q^{(0)}$ and $\mathcal{H}_D^{(0)}$ commute, a phenomenon which leads to the disappearance of terms proportional to $\omega_{Dr}^{(0)}\omega_{Qr}^{(0)}$ (Ref. 11).

With the following values of the factors $h^{(q)}$ (at exact resonance),[11]

$$h^{(0)}=\tfrac{1}{4}\,;\ h^{(1)}=0\,;\ h^{(2)}=\tfrac{3}{4}\,, \tag{2.20}$$

and the above definitions of spin and "lattice" correlation functions, in the limiting case of "strong" and "weak" collisions Eq. (2.11) may be simplified considerably.

B. Quadrupolar strong collisions

For $\tau_{cQ}\gg T_{mQ}$ the "lattice" correlation function $G_Q^{(0)}(t)$ in Eq. (2.11) remains in essence unchanged while $k_Q(t)$ decays to zero during quadrupolar thermal mixing. In practice, $k_Q(t)$ therefore vanishes at all times [see Eq. (2.14)] and we obtain

$$\left(\frac{1}{T_{1\rho}}\right)_Q=\frac{1}{4}\,\frac{\delta_Q}{\omega_1^2+\omega_{Dr}^2+\omega_{Qr}^2}\left(-\frac{dG_Q^{(0)}(t)}{dt}\right)_{t=0}\,. \tag{2.21}$$

If we define the *dynamical* quadrupolar local-field frequency (associated with that part of $\mathcal{H}_Q^{(0)}$ which fluctuates, thus causing spin-lattice relaxation) by [see Eqs. (2.17) and (2.13)]

$$(\omega_{Qr}^2)_{\mathrm{dyn}}=\frac{\delta_Q}{4}\frac{1}{N}\sum_{j=1}^{N}\sum_{k=1}^{N_d^{\mathrm{dyn}}}|V_{kj}^{(0)}(0)|^2$$
$$=\tfrac{1}{4}\,\delta_Q G_Q^{(0)}(0)\,, \tag{2.22}$$

we may formulate Eq. (2.21) also as follows:

$$\left(\frac{1}{T_{1\rho}}\right)=\frac{(\omega_{Qr}^2)_{\mathrm{dyn}}}{\omega_1^2+\omega_{Dr}^2+\omega_{Qr}^2}\,\frac{1}{G_Q^{(0)}(0)}\left(-\frac{dG_Q^{(0)}(t)}{dt}\right)_{t=0} \tag{2.23}$$

As illustrated earlier,[8,13] analogous to the theory of Rowland and Fradin[12] the factor on the right-hand side of Eq. (2.23) involving $G_Q^{(0)}(t)$ may be interpreted in terms of the average rate of change of the mobile part of the quadrupolar energy due to the jumps of mobile defects. Instead of the dynamical local-field precession frequency (2.22), equally well we could have inserted the *total* quadrupolar local-field precession frequency (2.17) into Eq. (2.21). The factor involving $G_Q^{(0)}(t)$ then would have to be interpreted in terms of the rate change of the *total* quadrupolar energy due to mobile-defect jumps.

C. Quadrupolar weak collisions

For $\tau_{cQ}\ll T_{mQ}$, $G_Q^{(0)}(t)$ decays much more rapidly than $k_Q(t)$. Hence, in Eq. (2.11) $k_Q(t)$ may be replaced by its initial value given by Eq. (2.14). After two subsequent partial integrations Eq. (2.11) then yields

$$\left(\frac{1}{T_{1\rho}}\right)_Q=\tfrac{3}{8}\,\delta_Q\,\frac{\omega_1^2+\alpha_Q[\omega_{Dr}^2+(\omega_{Qr}^{(n)})^2]}{\omega_1^2+\omega_{Dr}^2+(\omega_{Qr}^{(n)})^2}\,J_Q^{(0)}(2\Omega)\,, \tag{2.24}$$

where $J_Q^{(0)}(\omega)$ represents the spectral density associated with $G_Q^{(0)}(t)$:

$$J_Q^{(0)}(\omega) = 2\,\mathrm{Re}\int_0^\infty G_Q^{(0)}(t)e^{i\omega t}\,dt\ . \tag{2.25}$$

With $k_Q(t) \equiv 1$ the precession frequency (2.19) simplifies as follows:

$$\Omega^2 = \omega_1^2 + \omega_{Dr}^2 + (\omega_{Qr}^{(n)})^2 + 2\omega_{Dr}^{(0)}(\omega_{Dr}^{(n)} + \omega_{Qr}^{(n)}) + 2\omega_{Dr}^{(n)}\omega_{Qr}^{(n)}\ . \tag{2.26}$$

For $\omega\tau_{cQ} \ll 1$, $J_Q^{(0)}(\omega)$ is usually independent of ω (see, also, Sec. III A). The quantity

$$\alpha_Q = 1 + 2\,\frac{\omega_{Dr}^{(0)}(\omega_{Dr}^{(n)} + \omega_{Qr}^{(n)}) + \omega_{Dr}^{(n)}\omega_{Qr}^{(n)}}{\omega_{Dr}^2 + (\omega_{Qr}^{(n)})^2} \tag{2.27}$$

in Eq. (2.24) then represents the ratio of the quadrupolar relaxation rate in a vanishing rf field ($H_1 = \omega_1/\gamma = 0$) with respect to its value in a large field $\omega_1 \gg \omega_{Dr}, \omega_{Qr}$. Interestingly, if contrary to our earlier assumption the *dipolar* fluctuations in the crystal were of a *weak* and not of a strong-collision type, the secular part of $\mathcal{H}_D^{(0)}$ no longer would participate in the common spin temperature. $\omega_{Dr}^{(0)}$ would then vanish and α_Q would be closer to unity.

D. Extrapolation from strong to weak collisions

As we have seen above, the main difference between the strong-collision expression (2.21) and the weak-collision relationship (2.24) lies in the absence of thermal mixing between successive defect jumps in the weak-collision region. Accordingly, by extrapolating Eq. (2.21) towards weak collisions, the same result as that obtained from Eq. (2.24) for $\Omega\tau_{cQ} \gg 1$ is expected. To incorporate the absence of thermal mixing into Eq. (2.21), the following two considerations have to be applied: (i) The total heat capacity of the spin system has to be reduced by the secular quadrupolar contribution, i.e., ω_{Qr}^2 has to be replaced by $(\omega_{Qr}^{(n)})^2$ which, according to Eq. (2.17), is equal to $\frac{3}{4}\omega_{Qr}^2$. (ii) Fluctuations of the *secular* part of $\mathcal{H}_Q^{(0)}$ with respect to $\mathcal{H}_Z^r$ may no longer be communicated to $\mathcal{H}_D^{(0)}$ and $\mathcal{H}_{Zr}$. As a consequence, $G^{(0)}(t)$ has to be replaced by $\frac{3}{4}G_Q^{(0)}(t)$.[11] With these modifications Eq. (2.21) becomes

$$\left(\frac{1}{T_{1\rho}}\right)_Q = \frac{3}{16}\,\frac{\delta_Q}{\omega_1^2 + \omega_{Dr}^2 + \frac{3}{4}\omega_{Qr}^2}\left(-\frac{dG_Q^{(0)}(t)}{dt}\right)_{t=0} \tag{2.28}$$

If we use the fact that independent of the particular form of $G_Q^{(0)}(t)$, for $\Omega\tau_{cQ} \gg 1$ the spectral density and the first-time derivative of $G_Q^{(0)}(t)$ are related by[11]

$$J_Q^{(0)}(\Omega) = \frac{2}{\Omega^2}\left(-\frac{dG_Q^{(0)}(t)}{dt}\right)_{t=0}, \tag{2.29}$$

it is easily verified that Eq. (2.28) is identical with the result of Eq. (2.24) for $\Omega\tau_{cQ} \gg 1$. Comparing Eqs. (2.28) and (2.21), we readily see that the strong- and the weak-collision relaxation rates are connected as follows (at exact resonance):

$$\left(\frac{1}{T_{1\rho}}\right)_Q^{wc} = \frac{3}{4}\,\frac{\omega_1^2 + \omega_{Dr}^2 + \omega_{Qr}^2}{\omega_1^2 + \omega_{Dr}^2 + \frac{3}{4}\omega_{Qr}^2}\left(\frac{1}{T_{1\rho}}\right)_Q^{sc}\ . \tag{2.30}$$

Consequently, in zero field ($\omega_1 = 0$) the difference between the weak- and the strong-collision rate is the smaller the larger ω_{Qr} is with respect to ω_{Dr}. As ω_1 increases from zero so does the difference between $(T_{1\rho}^{-1})_Q^{wc}$ and $(T_{1\rho}^{-1})_Q^{sc}$. In the high-field limit this difference is accounted for by the factor of $\frac{3}{4}$. [Note that Eq. (2.30) implies that eventually activated *dipolar* fluctuations are of a strong-collision type.[14]]

In summary, if the strong-collision Rowland-Fradin type of expression for $(T_{1\rho}^{-1})_Q$ is known, the corresponding weak-collision expression is easily obtained by incorporating the above modifications. Since, generally, the weak-collision relaxation rate for $\Omega\tau_{cQ} \gg 1$ is smaller than the strong-collision result, the zero-field $(T_{1\rho}^{-1})_Q$ maximum must be wider than the corresponding weak-collision maximum which one would obtain if thermal mixing would not take place. This "strong-collision broadening of the usual weak-collision $(T_{1\rho}^{-1})_Q$ maximum is illustrated schematically in Fig. 1.

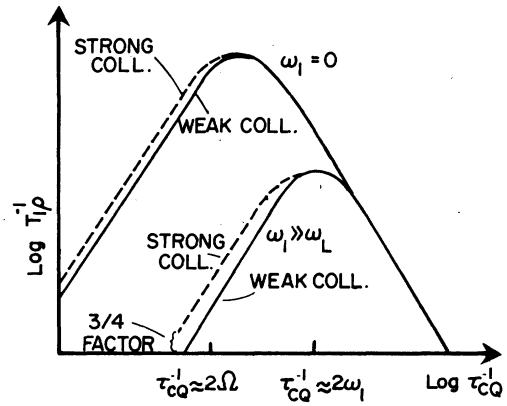

FIG. 1. Doubly logarithmic plot of the zero-field ($\omega_1 = 0$) and the high-field ($\omega_1 \gg \omega_L$) rate $(T_{1\rho}^{-1})_Q$ as a function of the defect jump rate τ_{cQ}^{-1} (schematical). The solid lines show the expected weak-collision $(T_{1\rho}^{-1})_Q$ maximum. For $\omega_1 = 0$ the breakdown of thermal mixing in the maximum region has to be taken into account. The dashed line indicates that a hypothetical zero-field maximum which lies entirely in the weak-collision region would be narrower than the actual maximum the two sides of which lie in the strong- and weak-collision region, respectively [see also Eq. (2.30)].

E. Relaxation in the transition region between strong and weak collisions

In contrast to the $(T_{1\rho})_Q$ minimum in a *large* rf field (which entirely lies in the weak-collision region), the low-field minimum of $(T_{1\rho})_Q$ appears in the transition region between weak and strong collisions. To determine this low-field minimum explicitly, the actual time and field dependence of $k_Q(t)$ in Eq. (2.11) has to be known.

The calculation of $k_Q(t)$ would involve a thorough understanding of the internal spin dynamics of the isolated spin system during quadrupolar thermal mixing. Since this is a very difficult task, at this point we are satisfied by guessing that the thermal-mixing process is characterized by the following simple exponential form of $k_Q(t)$:

$$k_Q(t) \approx e^{-t/T_{mQ}}. \tag{2.31}$$

Obviously, as easily verfied Eq. (2.31) satisfies the limiting conditions (2.14).

The next problem is to determine the frequency dependence of the thermal-mixing rate T_{mQ}^{-1}. Thermal-mixing processes are very similar to cross-relaxation processes in systems containing two spin species. Both require the presence of a nonsecular intermediary reservoir which allows two noninteracting spin reserviors (with commuting Hamiltonians) to interact *indirectly*. Similar to the exponential frequency dependence of the cross-relaxation rate observed[15] and interpreted[16] earlier, we therefore assume that

$$\frac{1}{T_{mQ}} \approx (\omega_{Dr}^2 + \omega_{Qr}^2)^{1/2} \exp \frac{-\omega_1}{(\omega_{Dr}^2 + \omega_{Qr}^2)^{1/2}}. \tag{2.32}$$

Equation (2.32) takes into account that in zero field ($\omega_1 = 0$) T_{mQ}^{-1} is to be identical with $(T_2^{\mathrm{RL}})^{-1} \approx (\omega_{Dr}^2 + \omega_{Qr}^2)^{1/2}$.

Inserting Eqs. (2.32) and (2.31) into the general relationships (2.11), (2.15), and (2.19), for a given form of $G_Q^{(0)}(t)$ the quadrupolar relaxation rate may be calculated in the entire region of interest. This includes the entire $(T_{1\rho})_Q$ minimum in a weak rf field (see Fig. 1) the properties (shape, width, etc.) of which, according to the above considerations, are a rather sensitive product of the assumptions (2.31) and (2.32).

III. "LATTICE" CORRELATION FUNCTIONS ASSOCIATED WITH DISLOCATION MOTION

By applying an external stress $\sigma(t)$ to a crystal, dislocations may be forced to move from one stabile position to another. The result is an anelastic or plastic contribution to the deformation $\epsilon(t)$ of the sample. As illustrated above, in order to determine the related nuclear-relaxation behavior, the corresponding quadrupolar "lattice"-correlation function $G_Q^{(0)}(t)$ has to be calculated for some assumed microscopic model of dislocation motion. Before deciding in favor of a particular type of deformation experiment, however, i.e., before choosing a specific mechanism of motion for the dislocations, in this section the general properties of quadrupolar and dipolar correlation functions associated with dislocation motion are investigated.

A. General form of quadrupolar "lattice" correlation functions

The usual procedure applied to determine correlation functions of the type of Eq. (2.13) begins with the conversion of the time average into an ensemble average. This step is only permitted, however, if the microscopic fluctuations causing the decay of $G_Q^{(0)}(t)$ represent a random *stationary* statistical process. In a discrete crystal lattice-dislocations perform discrete jumps. If the external stress $\sigma(t)$ varies in time, the mean time τ_d between such successive jumps of a given dislocation is a function of time. In general, the stress-induced dislocation motions, therefore, may not be considered as a *stationary* statistical process.

The time interval during which dislocation motion is investigated in a $T_{1\rho}$ experiment is the locking time t_l. The time average in Eq. (2.13), therefore, has to be extended over the time interval t_l,

$$\langle V_{kj}^{(0)}(t'+t) V_{k_j}^{(0)*}(t') \rangle_{t'} = \frac{1}{t_l} \int_0^{t_l} dt'\, V_{kj}^{(0)}(t'+t) V_{kj}^{(0)}(t'). \tag{3.1}$$

Owing to the nonstationarity of the underlying fluctuations, this time average may *not* simply be converted into an ensemble average.

A way to simplify the problem is to introduce a *mean* time $\bar{\tau}_d$ between successive dislocation jumps averaged over the locking time. If, then, the time variation of $\sigma(t)$ is such that $\bar{\tau}_d$ is actually independent of t_l, our goal is achieved in that the stress-induced dislocation motions may be considered to represent a *quasistationary* random process.

As an example, one may think of a periodic time variation of $\sigma(t)$

$$\sigma(t) = \sigma_0 \sin \omega_{\mathrm{def}} t, \tag{3.2}$$

where ω_{def} and σ_0 denote the deformation frequency and amplitude. If t_l is shorter than one deformation period, $T_{\mathrm{def}} = 2\pi/\omega_{\mathrm{def}}$, the value of $\bar{\tau}_d$ depends on the value of t_l. In contrast, in the limit in which $t_l \gg T_{\mathrm{def}}$, $\bar{\tau}_d$ is independent of t_l, and dislocation motion may be treated as a quasi-

stationary process. In the special case in which $\sigma(t)$ is time independent (such as in a plastic-deformation experiment), the above problem does not arise, and $\bar{\tau}_d$ is independent of t_l in all instances.

Assuming that a t_l-independent quantity $\bar{\tau}_d$ may be defined in a meaningful way, the time average in Eq. (2.13) may be converted into the following ensemble average[17]:

$$G_Q^{(0)}(t) = \frac{1}{N} \sum_{j=1}^{N} \sum_{k=1}^{N_d^{\mathrm{dyn}}} V_{kj}^{(0)}(\vec{r}_{kj}^{\,0}) \times \int_{\vec{r}} P_k(\vec{r},t) V_{kj}^{(0)}(\vec{r}_{kj}^{\,0} - \vec{r}) d\vec{r} . \tag{3.3}$$

With Fig. 2 the meaning of the vectors in Eq. (3.3) is easily understood: $\vec{r}_{kj}^{\,0}$ denotes the initial vector from an element of dislocation k to some spin j while $\vec{r}$ symbolizes the displacement vector of the same dislocation k in the slip direction.

$P_k(\vec{r},t)$ represents the probability that during time t dislocation k has been displaced by the vector $\vec{r}$ relative to its position at $t=0$. By assuming the probabilities $P_k(\vec{r},t)$ to be independent of $\vec{r}_{kj}^{\,0}$ (i.e., $P_k \equiv P$) it was implied that the relative motions of atoms and dislocations are uncorrelated. For atoms close to the path of the dislocation this is not quite true. However, since most atoms in the crystal do not perform any dislocation-induced jumps, the above approximation is well justified.

A realistic model of dislocation motion has to take into account that the displacement $\vec{r}$ results from a number of *discrete* jumps. Separating the time scale from the geometry associated with these jumps, similar to the self-diffusion case[17] we may write

$$P(\vec{r},t) = \sum_{S=0}^{\infty} w_S(t, \bar{\tau}_d(L)) P_S(\delta\vec{r}_S) \delta(\vec{r} - \delta\vec{r}_S) . \tag{3.4}$$

Here $w_S(t, \bar{\tau}_d(L))$ denotes the probability that some dislocation k of loop length L performs S discrete jumps in time t if the mean time between successive jumps (averaged over the locking time t_l) is $\bar{\tau}_d(L)$. Note that $\bar{\tau}_d$ assumes the same value for all dislocations with the same length. $P_S(\delta\vec{r}_S)$ represents the geometrical probability that as the result of S discrete jumps a dislocation has been displaced by the vector $\delta\vec{r}_S$ (see also Fig. 2). For reasons to become apparent below, $\delta\vec{r}_S$ was assumed to be independent of L.

The case for $S=0$ (i.e., no dislocation jumps during time t) requires some special attention. As discussed elsewhere,[18,19]

$$w_0(t, \bar{\tau}_d(L)) = 1 - \sum_{S=1}^{\infty} w_S(t, \bar{\tau}_d(L)) , \tag{3.5}$$

and the probabilities $P_0(\delta\vec{r}_0)$ vanish unless δr_0 vanishes and $P_0(0) = 1$.

Inserting Eq. (3.4) into (3.3) and converting the summation over individual dislocations k into an integration which involves the distribution $p(L)$ of loop lengths, we obtain

$$G_Q^{(0)}(t) = \frac{1}{N} \sum_{j=1}^{N_{\rho_m}} \int_{L=0}^{\infty} dL\, p(L) \bar{V}^{(0)}(r_j^0) \sum_{S=0}^{\infty} w_S(t, \bar{\tau}_d(L)) P_S(\delta\vec{r}_S) \bar{V}^{(0)*}(\vec{r}_j^{\,0} - \delta\vec{r}_S) , \tag{3.6}$$

where $\bar{V}^{(0)}(\vec{r}_j^{\,0})$ denotes the field gradient at the site $\vec{r}_j^{\,0}$ of spin j which originates from a unit element of a "representative" dislocation. The transition from $V_{kj}^{(0)}(\vec{r}_{kj}^{\,0})$ in Eq. (3.3) to $\bar{V}^{(0)}(\vec{r}_j^{\,0})$ implies that, per unit length, all dislocations are of the same type (e.g., edge or screw dislocations). With this assumption the EFG per unit dislocation length experienced by some spin j no longer depends on the dislocation k producing it, and the vector $\vec{r}_{kj}^{\,0}$ may formally be replaced by $\vec{r}_j^{\,0}$.

Also, as indicated in Eq. (3.6), the summation over all *spins* may then be simplified. As illustrated by Hut *et al.*,[4] this summation may be restricted to those N_{ρ_m} spins which actually experience a fluctuation of their EFG due to moving dislocations. If n_{ρ_m} is the number of such nuclei per unit dislocation length, $N_{\rho_m} = \rho_m V n_{\rho_m}$, where ρ_m and V denote the density of *mobile* dislocations and the crystal volume, respectively.

If, as usually assumed for ionic crystals and metals, on its way from one equilibrium position to another a dislocation travels approximately at the speed of sound, c_s, the actual time t_j a dislocation

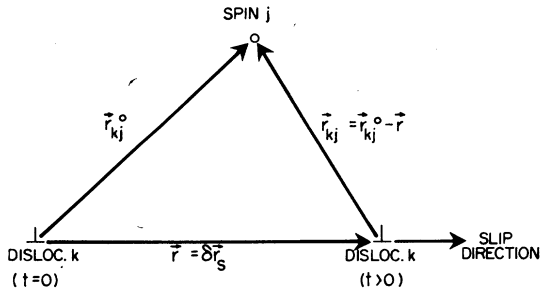

FIG. 2. Relative position of some spin j and a dislocation k at $t=0$ and at some later time t. In the time interval t the dislocation is assumed to have performed S jumps in the slip direction, thus being displaced by the vector $\vec{r} = \delta\vec{r}_S$. Consequently, the vector from an element of dislocation k to spin j has changed from $\vec{r}_{kj}^{\,0}$ to $\vec{r}_{kj}^{\,0} - \vec{r}$.

spends in the jumping process (the "actual jump time") is much shorter than its "mean waiting time" $\bar{\tau}_d(L)$ at an equilibrium position $[t_j \ll \bar{\tau}_d(L)]$. Also, in a statistical sense consecutive jumps of a dislocation are uncorrelated with each other, i.e., while resting, during the time $\bar{\tau}_d(L)$, a dislocation "forgets" all of its past history. As discussed by Argon,[20] the probabilities $w_S(t, \bar{\tau}_d(L))$ are therefore governed by the Poisson distribution

$$w_S(t, \bar{\tau}_d(L)) = \frac{1}{S!}\left(\frac{t}{\bar{\tau}_d(L)}\right)^S \exp\left(-\frac{t}{\bar{\tau}_d(L)}\right) . \quad (3.7)$$

If during a single jump a dislocation covers the distance $|\delta\vec{r}_1|$, the validity of Eq. (3.7) is limited by the following condition:

$$t_j \approx |\delta\vec{r}_1(L)|/c_S \ll \bar{\tau}_d(L) . \quad (3.8)$$

In typical plastic-deformation experiments $|\delta\vec{r}_1| \approx 10^{-4}$ cm independent of L. With $c_s \approx 10^5$ cm/sec we obtain $t_j \approx 10^{-9}$ sec, which is much less than typical values of $\bar{\tau}_d(L)$ which, in the minimum region of $(T_{1\rho})_Q$, are of the order of magnitude of 10^{-3} sec $\gtrsim \bar{\tau}_d(L) \gtrsim 10^{-5}$ sec. In an internal-friction experiment $|\delta\vec{r}_1|$ is of the order of one lattice constant ($\approx 10^{-8}$ cm). Consequently, $t_j \approx 10^{-13}$ sec and the validity of the Poisson distribution (3.7) is unquestioned.

The results of this section may be summarized by combing Eqs. (3.6) and (3.7) to yield

$$G_Q^{(0)}(t) = \frac{\rho_m V}{N}\sum_{S=0}^{\infty}\int_{L=0}^{\infty} dL\, p(L)\,\frac{B^{(0)}(S)}{S!} \times\left(\frac{t}{\bar{\tau}_d(L)}\right)^S \exp\left(-\frac{t}{\bar{\tau}_d(L)}\right) , \quad (3.9)$$

where the lattice sums $B^{(0)}(S)$ have been defined as follows:

$$B^{(0)}(S) = \sum_{j=1}^{n\rho_m} \bar{V}_j^{(0)}(\vec{r}_j^{\,0})\, P_S(\delta\vec{r}_S)\bar{V}_j^{(0)*}(\vec{r}_j^{\,0} - \delta\vec{r}_S) . \quad (3.10)$$

The Fourier transform and first time derivative of $G_Q^{(0)}(t)$ which dominate $(T_{1\rho}^{-1})_Q$ in the weak- and strong-collision region, respectively (see Secs. II B and II C), are easily found. Differentiating, at $t = 0$ we thus have

$$\left(-\frac{dG_Q^{(0)}(t)}{dt}\right)_{t=0} = \frac{\rho_m V}{N}\int_{L=0}^{\infty} dL\,\frac{p(L)}{\bar{\tau}_d(L)} \times[B^{(0)}(0) - B^{(0)}(1)] . \quad (3.11)$$

As illustrated for a similar case by Wolf,[18,19] with Eq. (3.9) the spectral densities (2.25) may be written as follows

$$J_Q^{(0)}(\omega) = \frac{1}{\omega}\,\frac{\rho_m V}{N}\sum_{S=0}^{\infty}\int_{L=0}^{\infty} dL\, p(L) B^{(0)}(S)\, j_S(\omega\bar{\tau}_d(L)) , \quad (3.12)$$

where[18,19]

$$j_S(x) = \mathrm{Re}[2x/(1-ix)^{S+1}] = \frac{2x}{(1+x^2)^{S+1}}\sum_{n=0}^{K}(-1)^n\binom{S+1}{2n}x^{2n} . \quad (3.13)$$

Here $x = \omega\bar{\tau}_d(L)$, and K is the greatest integer $\leq \frac{1}{2}(S+1)$.

For $S = 0$, $J_Q^{(0)}(\omega)$ represents the usual Lorentzian [obtained by assuming, on phenomenological grounds, $G_Q^{(0)}(t)$ to be simply exponential], since

$$j_0(x) = 2x/(1+x^2) . \quad (3.14)$$

For $S > 0$ the functions $j_S(x)$ have been analyzed elsewhere.[18,19] For later reference, it is pointed out that for $x \ll 1$

$$j_S(x) = 2x \quad (3.15)$$

for all values of S.

In concluding this section we recall that the microscopic mechanism of dislocation motion, except for the assumption of *discrete* dislocation jumps [see Eqs. (3.4) and (3.7)], has not been specified so far. Possible mechanisms encountered in different kinds of deformation experiments will be analyzed below. The remaining problem will be to express $\bar{\tau}_d(L)$ and, therefore, $(T_{1\rho}^{-1})_Q$ in terms of the plastic or anelastic sample deformation rate $\dot{\epsilon}(t) = f(\dot{\sigma}(t))$.

B. Dipolar "lattice" correlation functions

Whenever a dislocation changes its position in the crystal, the surrounding atoms have to move also. Therefore, in principle, dipolar and quadrupolar correlation functions are closely connected. For the following two reasons the dipolar lattice correlation function $G_D^{(0)}(t)$ and, hence, the dipolar contribution to the total spin-lattice relaxation rate (2.10) may be neglected as compared with $G_Q^{(0)}(t)$ and $(T_{1\rho}^{-1})_Q$, if the nuclear-spin relaxation is entirely due to dislocation motion.

(i) The mean time τ between successive dislocation-induced jumps of an arbitrary *atom* is much larger than $\bar{\tau}_d(L)$. The reason therefore is obvious: although a given *dislocation* may jump rather often during a given time interval, in a single dislocation jump only a fairly small number of *atoms* move slightly. By definition, however, τ is an averaged quantity for *all* atoms. Since the great majority of the atoms do not move at all during the deformation experiment, the value of τ averaged over all atoms of the sample is extremely long, and $G_D^{(0)}(t)$

decays considerably less fast than $G_Q^{(0)}(t)$.

(ii) Owing to the fact that the few atoms which ever "see" a dislocation pass by move by less than a lattice constant and then only in the very short time interval during which they are "visited" by a dislocation, the dipolar lattice sums $B_D^{(0)}(S)$ defined in analogy to Eq. (3.10) may practically by replaced by their rigid-lattice values $B_D^{(0)}(0)$. However, $G_D^{(0)}(t)$ then no longer decays in time[21] [i.e., $G_D^{(0)}(t) \equiv G_D^{(0)}(0)$] and $(T_{1\rho}^{-1})_D$ vanishes identically.

IV. RELAXATION BEHAVIOR FOR CONSTANT PLASTIC-DEFORMATION RATE

As discussed, for example, by Argon,[20] the mechanical behavior of crystalline material under the influence of a constant plastic-deformation rate $\dot{\epsilon}$ is governed by the Orowan equation[22]

$$\dot{\epsilon} = \phi b \rho_m v = \phi b \rho_m d_0/\tau_d . \tag{4.1}$$

The physical model underlying Eq. (4.1) assumes a thermally activated, jerky motion of the mobile dislocations of density ρ_m between the obstacles in the material. ϕ denotes a geometrical factor ($\phi \approx \frac{1}{2}$), while b symbolizes the magnitude of the Burgers vector. The mean dislocation velocity v may be expressed in terms of the mean distance d_0 between obstacles and the mean waiting time τ_d. In good approximation τ_d is independent of the dislocation loop length L.[20] Also, since $\dot{\epsilon}$ is constant, τ_d is time independent, and $\overline{\tau}_d \equiv \tau_d$, i.e., the time average over the locking time discussed in Sec. III A is irrelevant.

A. Relaxation rate in the strong-collision region

Because of the normalization condition $\int_0^\infty p(L)\,dL = 1$, the integration over L in Eq. (3.11) is now readily carried out and Eq. (4.1) may be applied to express ρ_m/τ_d in terms of $\dot{\epsilon}$. The remaining problem is to specify the probabilities $P_1(\delta\vec{r}_1)$ in the expression (3.10) for $B^{(0)}(1)$. Assuming an isotropic Gaussian distribution for the step width $\delta\vec{r}_1$, according to

$$P_1(\delta\vec{r}_1) = (2\pi)^{-1/2}\langle\delta r_1^2\rangle^{-1/2} \exp\left(-\frac{(\delta r_1 - d_0)^2}{\langle\delta r_1^2\rangle}\right), \tag{4.2}$$

where $\langle\delta r_1^2\rangle$ denotes the second moment of $P_1(\delta\vec{r}_1)$, Eq. (3.11) finally yields

$$\left(-\frac{dG^{(0)}(t)}{dt}\right)_{t=0} = \frac{\rho_m}{\tau_d}\Bigg[\int_{R=0}^{R_0}\int_{\theta=0}^{2\pi} R\,dR\,d\theta\,V^2(\vec{R}) - (2\pi)^{-1/2}\langle\delta r_1^2\rangle^{-1/2}\int_{R=0}^{R_0}\int_{\theta=0}^{2\pi} R\,dR\,d\theta\,V(\vec{R})\int^{\infty} d(\delta\vec{r}_1)\,V(\vec{R}-\delta\vec{r}_1)\exp\left(-\frac{(\delta r_1 - d_0)^2}{\langle\delta r_1^2\rangle}\right)\Bigg] . \tag{4.3}$$

In writing Eq. (4.3), the summation over spins in Eq. (3.10) has been converted into an integration over R and θ, thus taking into account that $V(\vec{R}) \equiv V_j^{(0)}(\vec{R})$ depends on R and θ only. The cutoff radius R_0 in Eq. (4.3) corresponds to the number of spins n_{ρ_m} appearing in Eq. (3.10). Analytic expressions for $V(\vec{R}) \equiv V(R,\theta)$ have been discussed by Kanert and Mehring[6] for $R > 3b$ (continuum range) and by Hut *et al.*[4] for the core of the dislocation ($R \leq 3b$).

As noted earlier,[4] in pure crystals the mean jump width d_0 of a dislocation is determined by the mean distance between the immobile (forest) dislocations which act as obstacles for the mobile dislocations. Typically, $d_0 \approx 10^{-4}$ cm. Since in the continuum approximation ($R > 3b$) $V(R)$ is proportional to R^{-1}, because of the large dislocation jump distances $V(|\vec{R} - \delta\vec{r}_1|) \approx 0$ and Eq. (4.3) reduces to

$$\left(-\frac{dG_Q(t)}{dt}\right)_{t=0} = \frac{\rho_m}{\tau_d}\int_0^{R_0}\int_0^{2\pi} V^2(R,\theta) R\,dR\,d\theta . \tag{4.4}$$

The integral appearing here represents the mean-squared EFG due to a dislocation element *of unit length*, usually written as $\langle V^2\rangle$. As shown by Hut *et al.* the value of $\langle V^2\rangle$ may either be determined theoretically or derived from the analysis of the measured rigid-lattice free-induction decay of the NMR signal.

Inserting (4.4) into (2.21), the quadrupolar relaxation contribution becomes

$$\left(\frac{1}{T_{1\rho}}\right)_Q = \frac{1}{4}\,\frac{\delta_Q\langle V^2\rangle}{\omega_1^2 + \omega_{Dr}^2 + \omega_{Qr}^2}\,\frac{\rho_m}{\tau_d} . \tag{4.5}$$

As pointed out earlier,[1-4] similar to the Orowan equation (4.1) the strong-collision relaxation rate (4.5) depends on the ratio ρ_m/τ_d. Combining Eqs. (4.1) and (4.5) we therefore obtain

$$\left(\frac{1}{T_{1\rho}}\right)_Q = \frac{1}{4}\,\frac{\delta_Q\langle V^2\rangle}{\omega_1^2 + \omega_{Dr}^2 + \omega_{Qr}^2}\,\frac{1}{\phi b d_0}\,\dot{\epsilon} , \tag{4.6}$$

Hence, for a given plastic-deformation rate $\dot{\epsilon}$ the nuclear spin-relaxation rate is proportional to the inverse mean-jump distance d_0^{-1}. This relationship may be used to determine d_0.[4,5]

B. Relaxation rate in the weak-collision region

As discussed above, in good approximation $V(\vec{r} - \delta\vec{r}_S)$ in Eq. (3.10) vanishes except for $S = 0$

when $\delta\vec{r}_S \equiv \delta\vec{r}_0$ is equal to zero. Consequently only rigid-lattice ($S=0$) terms contribute considerably to the spectral density $J_Q^{(0)}(\omega)$ given by Eq. (3.12). Then, if we insert Eqs. (3.12) and (3.10) into (2.24) and applying Eq. (3.14), the weak-collision relaxation rate may be written as follows

$$\left(\frac{1}{T_{1\rho}}\right)_Q = \tfrac{3}{4}\delta_Q\langle V^2\rangle \frac{\omega_1^2+\alpha_Q[\omega_{Dr}^2+(\omega_{Qr}^{(n)})^2]}{\omega_1^2+\omega_{Dr}^2+(\omega_{Qr}^{(n)})^2} \times \frac{\rho_m \tau_d}{1+4\Omega^2\tau_d^2}\ , \tag{4.7}$$

where α_Q and Ω are given by Eqs. (2.27) and (2.26) respectively. Substituting and applying the Orowan equation (4.1), for $\Omega\tau_d \gg 1$ from Eq. (4.7) we obtain

$$\left(\frac{1}{T_{1\rho}}\right)_Q = \tfrac{3}{16}\delta_Q \frac{\langle V^2\rangle}{\omega_1^2+\omega_{Dr}^2+(\omega_{Qr}^{(n)})^2} \frac{1}{\phi b d_0}\dot{\epsilon}\ . \tag{4.8}$$

As discussed in Sec. II E, Eq. (4.8) indeed represents the weak-collision limit of Eq. (4.6) in which (i) ω_{Qr}^2 has been replaced by $(\omega_{Qr}^{(n)})^2$ and (ii) the multiplicative factor $\frac{3}{4}$ has been introduced.

In the other extreme, for $\Omega\tau_d \ll 1$ Eq. (4.7) becomes

$$\left(\frac{1}{T_{1\rho}}\right)_Q = \tfrac{3}{4}\delta_Q\langle V^2\rangle \frac{\omega_1^2+\alpha_Q[\omega_{Dr}^2+(\omega_{Qr}^{(n)})^2]}{\omega_1^2+\omega_{Dr}^2+[\omega_{Qr}^{(n)}]^2} \times \phi b d_0 \rho_m^2 \frac{1}{\dot{\epsilon}}\ . \tag{4.9}$$

As is well known, the properties of the maximum of $(T_{1\rho}^{-1})_Q$ provide the most direct access to the understanding of the microscopic dynamic properties of the underlying mechanism of motion. Thus, the *position* of this maximum, governed by the relationship

$$2\Omega = \tau_d^{-1}\ , \tag{4.10}$$

leads to the mean dislocation jump rate, whereas the maximum *value* of $(T_{1\rho}^{-1})_Q$,

$$\left(\frac{1}{T_{1\rho}}\right)_Q^{\max} = \tfrac{3}{8}\delta_Q\langle V^2\rangle \frac{\omega_1^2+\alpha_Q[\omega_{Dr}^2+(\omega_{Qr}^{(n)})^2]}{\omega_1^2+\omega_{Dr}^2+(\omega_{Qr}^{(n)})^2} \frac{\rho_m}{\Omega}\ , \tag{4.11}$$

directly yields the density of *mobile* dislocations.[5]

The *total* dislocation density ρ_T may be extracted from the quadrupolar local-field precession frequency.[1-5] As dicussed by Kanert and Mehring,[6]

$$\omega_{Qr}^2 = A_0\rho_T\ , \tag{4.12}$$

where A_0 is a proportionality constant. Hence ω_{Qr}^2 is governed by the actual sample deformation ϵ. In contrast to ω_{Qr}^2, the *dipolar* local-field precession frequency ω_{Dr}^2 is constant and independent of any dislocation properties.

In concluding this section, Eqs. (4.7) and (2.26) may be extrapolated to the limit of large rf fields in which

$$\left(\frac{1}{T_{1\rho}}\right)_Q = \tfrac{3}{4}\delta_Q\langle V^2\rangle \frac{\rho_m \tau_d}{1+4\omega_1^2\tau_d^2}\ . \tag{4.13}$$

In contrast to the weak ω_1 dependence of $(T_{1\rho}^{-1})_Q$ for $\omega_1\tau_d \ll 1$ in a *small* rf field [see Eq. (4.9)], in the *high*-field limit $(T_{1\rho}^{-1})_Q$ is expected to be entirely independent of ω_1 if $\omega_1\tau_d \ll 1$. Owing to the assumption of the Poisson distribution (3.7), for $\omega_1\tau_d \gg 1$ Eq. (4.13) predicts the usual ω_1^{-2} dependence of the relaxation rate.

V. RELAXATION BEHAVIOR DURING INTERNAL-FRICTION EXPERIMENTS

A. Basic background on internal friction

The deformation amplitude in an internal-friction experiment is usually chosen such that during the entire deformation cycle all dislocations may be considered to be pinned by obstacles, such as impurity atoms or other dislocations. In a continuum approximation the stringlike vibration of dislocations under the influence of an external periodic stress $\sigma_{ext}(t)$ is governed by the Lücke-Granato-Koehler equation[23,24] (see also Fig. 3)

$$m_{eff}\ddot{x} + B\dot{x} - C\frac{\partial^2 x}{\partial y^2} = b\sigma(t)\ . \tag{5.1}$$

The effective dislocation mass m_{eff} per unit length is given by $m_{eff} = \pi b^2\rho$ (ρ: density of the material). B is a damping constant, while $C = 2Gb^2/\pi(1-\nu)$ (G: shear modulus; ν: Poisson's ratio). The variable x denotes the displacement of an element of dislocation line due to the resolved shear stress $\sigma(t)$, which represents the x component of $\sigma_{ext}(t)$ and is therefore usually written as $\sigma(t) = m\sigma_{ext}(t)$. m denotes the so-called Schmidt factor.[25] The y direction is defined by the unstrained "straight" dislocation line (see Fig. 3).

In a more microscopic model of Seeger *et al.*,[26,27] the discreteness of the crystal lattice is accounted for by assuming the thermal creation of double

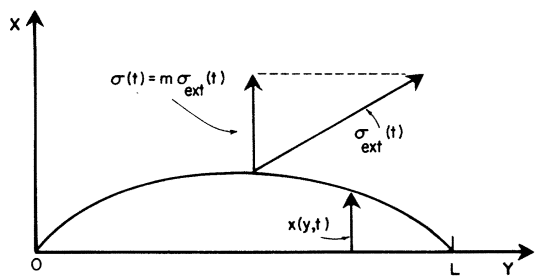

FIG. 3. Shape $x(y,t)$ of a dislocation of length L in the vibrating-string model (schematical). To obtain the resolved shear stress $\sigma(t)$, the external stress $\sigma_{ext}(t)$ has to be multiplied by the Schmidt factor m.

kinks. In this picture the discrete, stepwise motion of a pinned dislocation is determined by the periodic Peierls potential,

$$U(x) = (db/2\pi)\sigma_P\{1 - \cos[(2\pi/d)x]\}\,, \qquad (5.2)$$

while the dynamics of double kinks are governed by the diffusive motion in opposite directions of the two geometrical kinks which form it. In Eq. (5.2) d denotes the distance between neighboring Peierls barriers (in essence equal to the lattice constant). σ_P represents the Peierls stress which is typically of the order of $10^{-4}G$.

As illustrated by Engelke,[27] except for a small shift of the resonance frequency of a vibrating dislocation the rather complicated *"kink model"* in essence, leads to the same differential equation (5.1) as the simple *"string model."* Also, analogous to the discussion of Koehler[23] in both models the Poisson distribution

$$p(L) = (L/L_0^2)\, e^{-L/L_0} \qquad (5.3)$$

is assumed to govern the probability distribution of dislocation loop lengths. Here L_0 denotes the mean dislocation length obtained by averaging over all values of L in the entire crystal. Obviously, $p(L)$ satisfies the normalization condition $\int_0^\infty p(L)\,dL = 1$.

In the NMR–internal-friction experiments proposed here, the deformation frequency ω_{def} is much lower than the resonance frequency of a vibrating dislocation. (The latter varies typically between 10^6 and 10^8 sec^{-1}.) For what follows we shall assume this condition to be met.

Before applying the above models to predict the corresponding nuclear spin relaxation behavior, we observe that since dislocations may lie in different slip planes, the resolved shear stress $\sigma(t)$ acting on a dislocation depends on the Schmidt factor for a particular slip plane. In the general case the orientations of all possible slip directions with respect to the direction of the external stress and the corresponding densities of mobile and immobile dislocations in the different slip planes, therefore, have to be taken into account. For simplicity, the following considerations are restricted to the simple case in which m may assume a single value only. In two practical cases this assumption is well justified: (i) For cubic crystals containing only a small number of dislocations (i.e., for undeformed crystals) a direction of $\sigma_{ext}(t)$ may be chosen such that for all possible slip planes m assumes the same value or $m = 0$. As an example one may think of a ⟨100⟩ deformation in NaCl. (ii) For a high dislocation density in just one of the possible slip planes (produced by a single-slip deformation), the above simplifications are justified.

As discussed in Sec. III A, if the sample deformation rate $\dot{\epsilon}$ is *not* time dependent the underlying motion of dislocations does *not* represent a stationary statistical process. To overcome this difficulty we restrict ourselves to experiments in which the deformation period $T_{def} = 2\pi/\omega_{def}$ is much smaller than the locking time t_l. The dislocation motions as "seen" in a $T_{1\rho}$ experiment may then be treated as a quasistationary statistical process.

B. "Lattice" correlation function for the kink model

If discrete random dislocation jumps from one Peierls valley to an adjacent one are assumed, $G_Q^{(0)}(t)$ is determined by Eqs. (3.9) and (3.10).

To determine the mean time between successive jumps of a dislocation of length L, $\bar{\tau}_d(L) = T_{def}/\langle n(L)\rangle$, averaged over the locking time (or, for $t_l \gg T_{def}$, averaged over one deformation cycle, respectively), the mean number of jumps $\langle n(L)\rangle$ of a given dislocation in one deformation cycle has to be calculated. Since the shape of a deformed dislocation is fairly well described in terms of the string model,[27] the quasistatic solution of Eq. (5.1) may be used to show that

$$\langle n(L)\rangle = \frac{\bar{x}}{d} = \frac{1}{Ld}\int_0^L x(y)dy = \frac{1-\nu}{12dbG}\, L^2\sigma_0\,, \qquad (5.4)$$

where $\bar{x}$ denotes the mean deformation amplitude of a given dislocation of length L, and the resolved shear stress $\sigma(t) = \sigma_0 \sin\omega_{def} t$ was assumed to be a harmonic function of time. With Eq. (5.4) we may write

$$\bar{\tau}_d(L) = \frac{T_{def}}{\langle n(L)\rangle} = \frac{12dbG}{1-\nu}\,\frac{T_{def}}{\sigma_0 L^2} = U\,\frac{T_{def}}{\sigma_0 L^2}$$
$$= \frac{2\pi U}{\sigma_0 L^2 \omega_{def}} = \frac{U}{\sigma_0 L^2 f_{def}}\,, \qquad (5.5)$$

where U represents a proportionality constant and $f_{def} = \omega_{def}/2\pi$.

To evaluate the lattice sums $B^{(0)}(S)$ in Eqs. (3.9) and (3.10), the shape of a given dislocation has to be specified for any given value of S. The model applied below is illustrated schematically in Fig. 4. To obtain an order-of-magnitude estimate on the effect of internal friction on $(T_{1\rho}^{-1})_Q$, the following two simplifications have been incorporated into our model.

(i) The time required for the diffusive motion of a thermally created double kink is much shorter than $\bar{\tau}_d(L)$.[27] At a Larmor frequency close to the dislocation jump frequency this diffusion process is therefore "invisible" in a $T_{1\rho}$ experiment. Consequently, the microscopic mechanism and related time scale which transforms the dislocation, for example, from its position for $S = 0$ to its equilibrium position and shape for $S = 1$ (see Fig. 4)

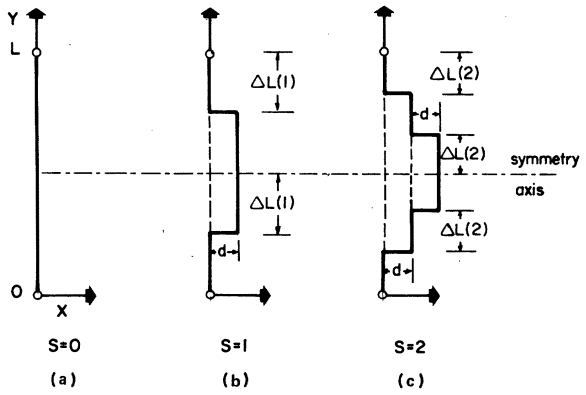

FIG. 4. Three equilibrium positions of a dislocation during internal friction in terms of a simple kink model: (a) before the first jump, i.e., in the undeformed crystal ($S=0$); (b) after one dislocation jump ($S=1$); and (c) after two dislocation jumps ($S=2$). In this simple model the entire shape after S jumps is completely characterized by the distance d between neighboring Peierls valleys and the quantity $\Delta L(S)=L/2(1+S)$.

does not enter into $G_Q^{(0)}(t)$.

(ii) For simplicity, the highly symmetric shape of a dislocation indicated in Fig. 4 is chosen. According to this model, for a given number of dislocation jumps the dislocation is subdivided into $2(1+S)$ segments of equal length $\Delta L(S)=L/2(1+S)$.

Owing to the discreteness of the dislocation motion, the probability $P_S(\delta\vec{r}_S)$ that due to S jumps any portion of the dislocation is displaced by the vector $\delta\vec{r}_S$ is given by

$$P_S(\delta\vec{r}_S)=\delta_{\vec{r}_S,S\vec{d}}\,, \tag{5.6}$$

where $\vec{d}$ denotes the unit jump vector while $\delta_{\vec{R},\vec{r}}$ represents Kronecker's delta in three dimensions. Hence, $P_S(\delta\vec{r}_S)$ vanishes unless $\vec{r}_S=S\vec{d}$ for which $P_S(\delta\vec{r}_S)=1$.

Analogous to Sec. IV A the summation in Eq. (3.10) involving nuclear spins may be converted into a volume integral [see, e.g., Eq. (4.3)]. Introducing again the EFG per unit dislocation length, $V(\vec{r})$, which depends on θ and r only (see Sec. IV A), and using Eq. (5.6), for the lattice sums (3.10) we obtain

$$B^{(0)}(S)=\frac{L}{(1+S)L_0}\sum_{k=0}^{S}H(k) \tag{5.7}$$

with

$$H(k)=\int_{R=0}^{R_0}\int_{\theta=0}^{2\pi}R\,dR\,d\theta\,V(\vec{R})V(\vec{R}-k\vec{d})\,. \tag{5.8}$$

Note that in contrast to the plastic-deformation case (see Sec. IV) $B^{(0)}(S)$ now depends on the dislocation length L.

As an example, in the isotropic-continuum approximation in which[6] $V(\vec{R})=AR^{-1}$ the function $H(k)$ becomes

$$H(k)=A^2\int_{R_c}^{R_0}\int_0^{2\pi}\frac{dR\,d\theta}{R(1+k^2d^2/R^2-2(kd/R)\cos\theta)^{1/2}}\,, \tag{5.9}$$

where R_c is the inner "cutoff radius" close to the core of the dislocation.

C. Kink model and strong collisions

Supposing all dislocations experience the same resolved shear stress $\sigma(t)$ [see (ii) in Sec. A above], it is clear that $\rho_m\equiv\rho_T$. Then, with Eqs. (5.4), (5.5), and (5.7), Eq. (3.11) yields

$$\left(-\frac{dG_Q^{(0)}(t)}{dt}\right)_{t=0}=\rho_T\,\frac{\sigma_0 f_{\rm def}}{UL_0^3}\,\{H(0)-\tfrac{1}{2}[H(0)+H(1)]\}\times\int_{L=0}^{\infty}dL\,L^4e^{-L/L_0}\,. \tag{5.10}$$

Since $d\ll R$, $H(1)$ may be expanded by writing $H(1)=H(0)-\delta H$. Hence, after integration over L, Eq. (5.10) becomes

$$\left(-\frac{dG_Q^{(0)}(t)}{dt}\right)_{t=0}=12\rho_TL_0^2\delta H\,\frac{\sigma_0 f_{\rm def}}{U}\,. \tag{5.11}$$

Equation (5.11) may be inserted into Eq. (2.21) to directly yield the strong-collision relaxation rate. Before inserting Eq. (5.11) into the relaxation rate (2.23), however, $G_Q^{(0)}(0)$ has to be determined. Combining Eqs. (3.9) and (5.7) we may write

$$G_Q^{(0)}(0)=\rho_TH(0)\int_{L=0}^{\infty}\frac{dL}{L_0}\,\frac{L^2}{L_0^2}\,e^{-L/L_0}=2\rho_TH(0)\,. \tag{5.12}$$

Inserting into Eq. (2.23) we finally obtain

$$\left(\frac{1}{T_{1\rho}}\right)_Q=\frac{\omega_{Qr}^2}{\omega_1^2+\omega_{Dr}^2+\omega_{Qr}^2}\,\frac{1-\nu}{2}\times\frac{\delta H}{H(0)}\,\frac{\sigma_0}{G}\,\frac{L_0^2}{db}\,f_{\rm def}\,, \tag{5.13}$$

where it was taken into account that, since all dislocations are mobile, $(\omega_{Qr}^2)_{\rm dyn}\equiv\omega_{Qr}^2$.

Starting from Eq. (5.9), in the approximation that $d\ll R$, $H(0)$ and δH may be determined in terms of the isotropic-continuum approximation. After straightforward calculation one finds (for $R_0\gg R_c$)

$$H(0)=2\pi A^2\ln(R_0/R_c);\quad \delta H=\tfrac{1}{2}\pi A^2(d^2/R_c^2)\,. \tag{5.14}$$

Inserting into Eq. (5.13) we thus obtain

$$\left(\frac{1}{T_{1\rho}}\right)_Q=\frac{\omega_{Qr}^2}{\omega_1^2+\omega_{Dr}^2+\omega_{Qr}^2}\,\frac{1-\nu}{8\ln(R_0/R_c)}\times\frac{d^2}{R_c^2}\,\frac{\sigma_0}{G}\,\frac{L_0^2}{db}\,f_{\rm def}\,. \tag{5.15}$$

To estimate the magnitude of this relaxation rate, let us consider an internal-friction–NMR experiment in ^{23}NaCl. For small values of ω_1 the heat-capacity ratio $\omega_{Qr}^2/(\omega_1^2+\omega_{Dr}^2+\omega_{Qr}^2)$ is approximately equal to $\frac{1}{2}$ (Ref. 4). Then, with the values $R_c \approx 3d$, $R_0 = L_0 \approx 10^{-4}$ cm, $b \approx 4\times 10^{-8}$ cm, $d \approx 3\times 10^{-8}$ cm, $G = 2\times 10^6$ N/cm^2, $\sigma_0 \approx 100$ N/cm^2 (i.e., $\sigma_0/G = 0.5\times 10^{-4}$), and $1-\nu \approx 0.7$, Eq. (5.15) yields

$$\left(\frac{1}{T_{1\rho}}\right)_Q \approx \frac{\omega_{Qr}^2}{\omega_1^2+\omega_{Dr}^2+\omega_{Qr}^2}\ \tfrac{1}{2} f_{\rm def} \approx \tfrac{1}{4} f_{\rm def}\,. \quad (5.16)$$

The "background" (deformation-independent) relaxation rate in ^{23}NaCl is of the order of 0.1 sec^{-1}. Consequently, a deformation frequency $f_{\rm def}$ of only a few cycles per second should result in a measurable change of the relaxation rate.

D. Kink model and weak collisions

With Eqs. (5.3) and (5.7) the spectral density (3.12) now becomes

$$J_Q^{(0)}(\omega) = \frac{\rho_T}{\omega L_0^3}\int_{L=0}^{\infty} dL\, L^2 e^{-L/L_0} \times \sum_{S=0}^{\infty}\frac{1}{1+S}\sum_{k=0}^{S} H(k) j_S(\omega\bar{\tau}_d(L))\,. \quad (5.17)$$

In practice the summation over the number S of dislocation jumps may be limited to the average number of jumps of a dislocation during a quarter of a deformation cycle.

To evaluate $J_Q^{(0)}(\omega)$ in its entire maximum region the lattice sums $H(k)$ have to be computed. Since this is a rather lengthy numerical task, in the rest of this section we will briefly discuss some properties of $J_Q^{(0)}(\omega)$ which may be derived analytically. Thus, by inserting Eqs. (5.17) and (3.13) into Eq. (2.24), the general properties of $(T_{1\rho}^{-1})_Q$ may be derived. As in Sec. IV B, in the usual two extreme regions analytical expressions for $(T_{1\rho}^{-1})_Q$ are readily obtained.

First, for $\Omega\bar{\tau}_d(L) \ll 1$ Eqs. (3.15), (5.17), and (2.24) may be combined to yield

$$\left(\frac{1}{T_{1\rho}}\right)_Q = (\omega_{Qr}^{(n)})^2\ \frac{\omega_1^2+\alpha_Q[\omega_{Dr}^2+(\omega_{Qr}^{(n)})^2]}{\omega_1^2+\omega_{Dr}^2+(\omega_{Qr}^{(n)})^2} \times \frac{48F}{1-\nu}\ \frac{db}{L_0^2}\frac{G}{\sigma_0}\frac{1}{f_{\rm def}}\,, \quad (5.18)$$

where the factor F was defined via the relationship

$$\sum_{S=0}^{\infty}\frac{1}{1+S}\sum_{k=0}^{S} H(k) = H(0)\sum_{S=0}^{\infty}\frac{1}{1+S}\sum_{k=0}^{S}\frac{H(k)}{H(0)} = FH(0)\,, \quad (5.19)$$

and $(\omega_{Qr}^{(n)})^2$ was introduced by [see Eqs. (2.17) and (5.8)]

$$(\omega_{Qr}^{(n)})^2 = \tfrac{3}{16}\,\delta_Q H(0)\rho_T\,. \quad (5.20)$$

Second, for $\Omega\bar{\tau}_d(L) \gg 1$, rather than following the above outline, the strong-collision expression (5.13) or (5.15), respectively, may be modified by (i) replacing ω_{Qr}^2 by $(\omega_{Qr}^{(n)})^2$ and (ii) multiplying the right-hand side of Eq. (5.13) or (5.15) by $\frac{3}{4}$. By comparing, e.g., Eqs. (5.18) and (5.13), the opposite variations of $(T_{1\rho}^{-1})_Q$ as a function of $L_0^2\sigma_0 f_{\rm def}$ on the two sides of the $(T_{1\rho}^{-1})_Q$ maximum are observed. The quadratic dependence of $(T_{1\rho}^{-1})_Q$ on the mean dislocation length L_0 enables NMR measurements of L_0 as a function, for example, of radiation effects ("pinning studies").

For $\Omega\bar{\tau}_d(L) \gg 1$, $(T_{1\rho}^{-1})_Q$ is a fairly insensitive function of the microscopic mechanism of dislocation motion. In contrast, the value of $(T_{1\rho}^{-1})_Q$ for $\Omega\bar{\tau}_d(L) \ll 1$, via the value of F, depends strongly on the convergence of the summation over S in Eq. (5.19), i.e., on the model assumed for the shape of the dislocation during its motion (see Fig. 4). It is hence obvious that both the *width* and the *position* of the $(T_{1\rho}^{-1})_Q$ maximum contain information on the microscopic mechanism of dislocation motion during internal friction. To determine position, width, and depth of the $(T_{1\rho}^{-1})_Q$ maximum analytically, the factors $H(k)$ have to be computed in terms of a model such as, e.g., the one underlying Fig. 4.

As a rough estimate the *position* of the maximum of $(T_{1\rho}^{-1})_Q$ appears whenever the condition

$$2\Omega \approx \langle \bar{\tau}_d^{-1}(L)\rangle_L \quad (5.21)$$

is satisfied. The mean dislocation jump rate averaged over the entire distribution of loop lengths may be determined from the relationship [see Eqs. (5.3) and (5.5)]

$$\langle \bar{\tau}_d^{-1}(L)\rangle_L = \int_0^{\infty}\frac{1}{\bar{\tau}_d(L)}p(L)\,dL = \frac{1-\nu}{2}\frac{L_0^2}{db}\frac{\sigma_0}{G} f_{\rm def}\,. \quad (5.22)$$

For ^{23}NaCl, in zero field Ω is of the order of 10^4 sec^{-1} [see Eq. (2.26)]. With the values of the relevant parameters listed in Sec. C above inserted into Eqs. (5.21) and (5.22), the maximum of $(T_{1\rho}^{-1})_Q$ is expected for a deformation frequency $f_{\rm def}$ of about 150 sec^{-1}.

E. Relaxation behavior for the vibrating-string model

As outlined in Sec. V A, the motion of a dislocation in a continuous medium exposed to a periodic stress $\sigma(t)$ is governed by Eq. (5.1). For sinusoidal stress $\sigma(t) = \sigma_0 \sin\omega_{\rm def} t$ the solution of Eq. (5.1) which satisfies the boundary conditions indicated in Fig. 3 reads as follows[23-25]:

$$x(y,t)=\frac{\pi(1-\nu)\sigma_0}{4Gb}(Ly-y^2)\sin\omega_{def}t\,. \tag{5.23}$$

In contrast to the *discrete* dislocation jumps assumed in the kink model, Eq. (5.23) describes the *continuous* stringlike vibration of dislocations. As illustrated now, this leads to significantly different forms of the quadrupolar "lattice" correlation function $G_Q^{(0)}(t)$ for the two models.

To calculate $G_Q^{(0)}(t)$ for the string model, we have to go back to Eq. (3.3) which is valid if the locking time t_l is much larger than a deformation period T_{def}. Due to the absence of any randomness in the dislocation motion (which is now completely predetermined) Eq. (3.4) is no longer valid. Instead, the probability $P_k(\vec{r},t)$ that during time t some dislocation k of length L has been displaced by the vector $\vec{r}$ is now given by

$$P_k(\vec{r},t)=\delta(\vec{r}-\vec{r}_L(y,t))\,, \tag{5.24}$$

where $\vec{r}_L(y,t)$ denotes the displacement vector of this dislocation, which depends on the position y, of course [see Fig. 3 and Eq. (5.23)]. Since all dislocations k with equal length L experience identical displacements, $\vec{r}_L(y,t)$ is a function of L but no longer of the particular dislocation k.

As illustrated in Secs. IV A and V B, the summations in Eq. (3.3) over all spins and dislocations may be converted into (i) a volume integration $(\vec{R},\theta)$; and (ii) an integration of all EFG's $V(\vec{R}-\vec{r}_L(y,t))$ per unit dislocation length over all dislocations, respectively (L,y). Hence, with Eq. (5.24), from Eq. (3.3) we obtain

$$G_Q^{(0)}(t)=\rho_T\int_{R=0}^{R_0}\int_{\theta=0}^{2\pi}R\,dR\,d\theta\,V(\vec{R})\int_{L=0}^{\infty}p(L)\,dL \times\int_{y=0}^{L}dy\,V(\vec{R}-\vec{r}_L(y,t))\,, \tag{5.25}$$

where, as above, it was assumed that $\rho_m\equiv\rho_T$ [see (ii) in Sec. V A].

To gain some qualitative insight into the expected relaxation behavior, again we apply the continuum approximation in which $V(\vec{R})=AR^{-1}$; then

$$G_Q^{(0)}(t)=A^2\rho_T\int_{L=0}^{\infty}p(L)\,dL\int_{y=0}^{L}dy\int_{R=R_c}^{R_0}\int_{\theta=0}^{2\pi}\frac{dR\,d\theta}{1+x^2(y,t)/R^2-[2x(y,t)/R]\cos\theta}\,. \tag{5.26}$$

Here it was noted that $|\vec{r}_L(y,t)|$ is identical with $x(y,t)$ given by Eq. (5.23). Since the majority of all spins is located far away from a vibrating dislocation, for the approximate determination of the bulk relaxation behavior the denominator on the right-hand side of Eq. (5.26) may be expanded for $x(y,t)\ll R$ (see also Sec. V C), and we obtain $(R_0\gg R_c)$

$$G_Q^{(0)}(t)=A^2\rho_T\int_{L=0}^{\infty}p(L)dL\int_{y=0}^{L}dy\left(2\pi\ln\frac{R_0}{R_c}-\frac{\pi}{2}\frac{x^2(y,t)}{R_c^2}\right). \tag{5.27}$$

Inserting Eqs. (5.23) and (5.3), the remaining two integrations may be carried out to yield

$$G_Q^{(0)}(t)=4\pi\rho_T A^2L_0[\ln(R_0/R_c)-D\sin^2\omega_{def}t]\,, \tag{5.28}$$

where

$$D=3\frac{L_0^4}{R_c^2}\left(\frac{\pi(1-\nu)\sigma_0}{4Gb}\right)^2. \tag{5.29}$$

The form (5.28) of $G_Q^{(0)}(t)$ derived for the string model corresponds to Eqs. (3.9) and (5.7) which were obtained for the kink model. To gain some qualitative understanding of the relaxation behavior which follows from Eq. (5.28), let us determine its Fourier transform (2.25). Using the complex-exponential representation of $\sin\omega_{def}t$ together with the definition of Dirac's delta function,

$$\sin^2(\omega_{def}t)=-\tfrac{1}{4}(e^{2i\omega_{def}t}+e^{-2i\omega_{def}t})+\tfrac{1}{2}\,, \tag{5.30}$$

$$\mathrm{Re}\int_0^{\infty}dt e^{i\omega t}=\pi\delta(\omega)\,, \tag{5.31}$$

the spectral density (2.25) becomes

$$J_Q^{(0)}(\omega)=8\pi^2\rho_T A^2L_0\{[\ln(R_0/R_c)-\tfrac{1}{2}D]\delta(\omega) +\tfrac{1}{4}D[\delta(\omega+2\omega_{def})+\delta(\omega-2\omega_{def})]\}. \tag{5.32}$$

Equation (5.32) may finally be inserted into Eq. (2.24) to obtain the weak-collision relaxation rate $(T_{1\rho}^{-1})_Q$. Interestingly, $(T_{1\rho}^{-1})_Q$ does *not* show a maximum, which is in sharp contrast to all cases in which the fluctuations of the spin-lattice interaction (2.9) represent a *random* statistical process. Instead, for $\Omega=0$ and $|\Omega|=\omega_{def}$, $(T_{1\rho}^{-1})_Q$ is predicted to become infinite while it vanishes for all other values of Ω. [Because of the local-field contributions in Eq. (2.26) Ω never vanishes. Hence, the first term in the bracket of Eq. (5.32) is irrelevant.]

The physical origin of the absence of a $(T_{1\rho}^{-1})_Q$ maximum lies in the fact that within the framework of the vibrating-string model all dislocations move coherently. Consequently, $J_Q^{(0)}(\omega)$ peaks

sharply at the corresponding frequency of the coherent vibrations and vanishes otherwise. If a randomness in the time scale on which different dislocation jumps take place were added, the spectrum of $J_Q^{(0)}(\omega)$ would become broader and it would show a maximum. The peaking of Eq. (5.32) for $|\omega| = 2\omega_{\rm def}$ and *not* for $|\omega| = \omega_{\rm def}$ indicates that the characteristic time between two successive fluctuations of the quadrupolar spin-dislocation interaction is *half* a deformation period and not a full period. This appears physically reasonable since in the turning points (i.e., after every time interval $\frac{1}{2}T_{\rm def}$) the dislocation comes to a full rest.

VI. RELAXATION FOR INTERMEDIATE DEFORMATION AMPLITUDES

If the amplitude σ_0 of the periodic stress acting on a dislocation becomes larger than some critical value, the dislocation may break loose from its pinning points. If a sufficiently large number of dislocations may be depinned, the mechanical behavior of the crystal may be dominated entirely by these "mobile" dislocations (in the sense of Sec. IV), and the effect of the pinned dislocations is negligible. Before we discuss the NMR relaxation behavior for the general case (partial unpinning), let us first consider the extreme in which the mechanical properties are entirely dominated by the unpinning of dislocations.

A. Large deformation amplitudes: fatigue

During a fatigue experiment the microscopic behavior of dislocations is very similar to their dynamical properties in an elastic-deformation experiment (see Sec. IV). However, while in the latter the crystal is deformed (usually for a short time interval only) at a constant strain rate $\dot\epsilon$, in a fatigue experiment $\dot\epsilon$ is a periodic function of time and the external stress usually acts for a much longer time. This leads to a time variation of the fraction ρ_m/ρ_T and the mean step width d_0.

As in Sec. V, we assume that the deformation period is much shorter than the locking time. Via the Orowan equation (4.1) it is then possible to define a quasistationary mean time $\langle\tau_d\rangle$ between successive jumps of a dislocation by performing a time average over the absolute value of $\dot\epsilon(t)$,

$$\langle|\dot\epsilon(t)|\rangle = \frac{1}{T_{\rm def}}\int_0^{T_{\rm def}} |\dot\epsilon(t)|\,dt$$

$$= (2/\pi)\dot\epsilon(0) = \phi b\rho_m(d_0/\langle\tau_d\rangle)\,. \qquad (6.1)$$

Comparing with Eq. (4.1), we find that

$$1/\langle\tau_d\rangle = (2/\pi)\ (1/\tau_d)\,, \qquad (6.2)$$

where τ_d is the mean waiting time of a dislocation in a plastic-deformation experiment ($\dot\epsilon$ = constant). Replacing Eq. (4.1) by Eq. (6.1), all results of Sec. IV remain valid for the interpretation of NMR-fatigue experiments. In practice, such experiments are expected to yield information on the time dependence of quantities such as the density ρ_m of mobile dislocations, the step width d_0 (i.e., the mean distance between obstacles), and the internal dislocation dynamics ($\langle\tau_d\rangle$).

B. Intermediate deformation amplitudes: partial unpinning

For simplicity, let us assume that all pinning points are identical, i.e., that all of them may be characterized by the same value of the "critical depinning force" $f_{\rm cr}$ which has to be overcome for a dislocation to break loose and thus to be "mobile" in the sense of Sec. IV. Since the external force acting on a dislocation is proportional to its loop length L, a given value of $f_{\rm cr}$ corresponds to a certain critical length $L_{\rm cr}$. According, for example, to Eq. (5.1), the two quantities are related as

$$f_{\rm cr} = b\,L_{\rm cr}\sigma_0\,. \qquad (6.3)$$

Hence, for a given resolved shear stress $\sigma(t) = \sigma_0 \sin\omega_{\rm def}t$ all dislocations for which $L > L_{\rm cr}$ may be displaced by large distances. Their relaxation behavior has been discussed in Sec. VIA above. In contrast, all dislocations with $L \le L_{\rm cr}$ remain pinned and show a relaxation behavior which is characteristic for internal-friction experiments (see Sec. V).

To determine the resulting nuclear spin-relaxation behavior, the integrations over L in Eqs. (3.9), (3.11), and (3.12) have to be subdivided into the two intervals, $0 \le L \le L_{\rm cr}$ and $L_{\rm cr} < L < \infty$. Also, because of the different mechanisms of dislocation motion in the two regions, $B^{(0)}(S)$ and $\bar\tau_d(L)$ have to be properly identified with their forms derived in Secs. V and IV, respectively.

Owing to the existence of two different mean waiting times, $\langle\tau_d\rangle$ and $\bar\tau_d(L)$, in the general case strong and weak collisions have to be distinguished for either dislocation jumping mechanism. For simplicity, we shall only consider two of the four extreme cases.

If both $\bar\tau_d(L)$ and $\langle\tau_d\rangle$ satisfy their respective strong-collision condition [$\langle\tau_d\rangle, \bar\tau_d(L) \gg T_{mQ}$, see also Sec. IIB], the results of Secs. IVA and VC may be combined to yield [see Eqs, (4.6), (6.1), (5.10), and (2.21)]

$$\left(\frac{1}{T_{1\rho}}\right)_Q=\frac{1}{4}\frac{\delta_Q}{\omega_1^2+\omega_{Dr}^2+\omega_{Qr}^2}\left(\pi_{\rm dep}\frac{\langle V^2\rangle\langle|\dot{\epsilon}(t)|\rangle}{\phi b d_0}+\frac{1-\nu}{24}\rho_T\delta H\frac{L_0^2}{db}\frac{\sigma_0}{G}f_{\rm def}\right.$$
$$\left.\times\left\{-e^{-L_{\rm cr}/L_0}\left[\left(\frac{L_{\rm cr}}{L_0}\right)^4+4\left(\frac{L_{\rm cr}}{L_0}\right)^3-12\left(\frac{L_{\rm cr}}{L_0}\right)^2+24\left(\frac{L_{\rm cr}}{L_0}-1\right)\right]\right\}\right). \tag{6.4}$$

Here, $\pi_{\rm pin}$ and $\pi_{\rm dep}$ denote the percentage of all dislocations that are pinned and depinned, respectively. Starting from the normalization condition (see Sec. V A)

$$\int_0^\infty p(L)\,dL=\int_0^{L_{\rm cr}}p(L)\,dL+\int_{L_{\rm cr}}^\infty p(L)dL=\pi_{\rm pin}+\pi_{\rm dep}=1\,, \tag{6.5}$$

for example $\pi_{\rm dep}$ is given by [see also Eq. (5.3)]

$$\pi_{\rm dep}=\int_{L_{\rm cr}}^\infty\frac{dL}{L_0}\frac{L}{L_0}e^{-L/L_0}=\left(1+\frac{L_{\rm cr}}{L_0}\right)e^{-L_{\rm cr}/L_0}\,, \tag{6.6}$$

while $\pi_{\rm pin}$ may be calculated from the normalization condition (6.5). It should be kept in mind that these relations have been derived with the assumption that all pinning points are characterized by the same value of the critical depinning force $f_{\rm cr}$.

The weak-collision expression for $(T_{1\rho}^{-1})_Q$ may be derived similarly. Thus, combining Eqs. (4.7), (5.17), and (2.24) we obtain

$$\left(\frac{1}{T_{1\rho}}\right)_Q=\frac{3}{4}\delta_Q\rho_T\frac{\omega_1^2+\alpha_Q[\omega_{Dr}^2+(\omega_{Qr}^{(n)})^2]}{\omega_1^2+\omega_{Dr}+(\omega_{Qr}^{(n)})^2}\left(\frac{\pi_{\rm dep}\langle\tau_d\rangle}{1+4\Omega^2\langle\tau_d\rangle^2}+\pi_{\rm pin}\frac{1}{4\Omega L_0^3}\int_{L=0}^{L_{\rm cr}}dL\,L^2e^{-L/L_0}\sum_{S=0}^{\infty}\frac{1}{1+S}\sum_{k=0}^{S}H(k)j_S(2\Omega\bar{\tau}_d(L))\right). \tag{6.7}$$

According to Eq. (6.7), $(T_{1\rho}^{-1})_Q$ in essence represents a weighted superposition of the two relaxation contributions discussed in Secs. IV B and V D. Hence, in the general case $(T_{1\rho}^{-1})_Q$ may show two maxima (see Fig. 5). The one appearing for $2\Omega\approx\langle\tau_d^{-1}\rangle$ is due to longer-range migration of *depinned* dislocations while the other, which appears whenever $2\Omega\approx\langle\bar{\tau}_d^{-1}(L)\rangle$, arises from the stringlike vibration of the *pinned* dislocations. Since $\langle\tau_d\rangle$ and $\langle\bar{\tau}_d(L)\rangle$ may differ considerably, a shift of the $(T_{1\rho}^{-1})_Q$ maximum towards longer τ values (i.e., larger deformation frequencies) is expected as the amplitude σ_0 of the resolved shear stress is increased in such a way to produce a transition from an internal-friction to a fatigue experiment. This transition is illustrated schematically in Fig. 5. The heights of the two maxima shown are directly related to the densities of pinned and depinned dislocations, respectively.

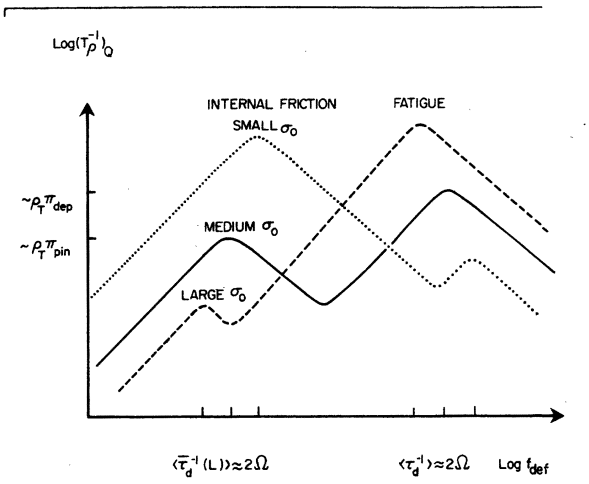

FIG. 5. Doubly logarithmic plot of the quadrupolar relaxation rate versus deformation frequency in a mixed internal friction-fatigue–NMR experiment (schematical). The $(T_{1\rho}^{-1})_Q$ maximum associated with the depinned dislocations appears whenever $\langle\tau_d^{-1}\rangle\approx 2\Omega$ (see Sec. IV A), while the maximum for the pinned dislocations is reached for $\langle\tau_d^{-1}(L)\rangle\approx 2\Omega$ [see Eq. (5.21)]. For large stress amplitude σ_0, in both internal-friction and fatigue experiments a dislocation performs more jumps per deformation cycle than for small stress amplitude. This is the reason for the shift of the maxima towards lower frequencies as σ_0 is increased. Simultaneously, more dislocations may break loose from their pinning points, which results in an increase of the $(T_{1\rho}^{-1})_Q$ value at the fatigue maximum and a corresponding decrease in the internal-friction maximum. $\pi_{\rm dep}$ and $\pi_{\rm pin}$ have been defined in Eqs. (6.5) and (6.6).

VII. CONCLUDING REMARKS ON THE ROLE OF SPIN DIFFUSION

The basic relaxation theory discussed in Sec. II and, hence, the main conclusions of this article are only valid if a common spin temperature may be assigned to the entire spin system imbedded in a crystal. As we have seen, the thermal mixing between Zeeman and the secular dipole or quadrupole spin reservoir allows separation of "strong" and "weak" collisions, but the validity of the single-spin-temperature assumption is practically not affected by such thermal-mixing processes.

The establishment of a common spin temperature of the entire crystal following, for example, a nuclear or dislocation jump requires the communication of spins located in different parts of the sample. This communication may be established by spin diffusion (i.e., the transport of magnetization without transport of mass) or by the bodily motion of spins or dislocations themselves.[28]

In an internal-friction experiment only very few spins are directly disturbed by the stringlike vibration of the dislocation. (Their number is proportional to the area in the crystal covered by the vibrating dislocation.) Since most spins never "see" a dislocation pass by, spin diffusion from the disturbed area to the bulk spins is vital in distributing the relaxing spin temperature uniformly all over the crystal. If spin diffusion is not rapid enough to ensure the existence of a uniform spin temperature in the entire crystal at all times, the relaxation rate of the bulk spins is reduced as discussed by Moran and Lang.[28] In the limit in which no spin diffusion takes place at all, the vibrating dislocation keeps disturbing the very same spins at all times without the bulk spins ever experiencing a disturbance of their precession frequency. Experimentally, such a situation is encountered if the sample deformation frequency ω_{def} is made very large.[29]

If the dislocations may migrate over large distances (as, e.g., in a plastic-deformation experiment), the communication between spatially separated spins is enhanced considerably. Consequently, possible spin-diffusion limitations of $(T_{1\rho}^{-1})_Q$ are not as serious as in internal-friction experiments in which the spin system is disturbed in a much more localized manner.

A quantitative treatment of the effect of spin diffusion in the presence of quadrupolar interactions on the properties of $(T_{1\rho}^{-1})_Q$ is a very difficult task.[28] By choosing a small enough sample deformation frequency ω_{def}, however, no spin-diffusion limitation effects on $(T_{1\rho}^{-1})_Q$ are expected. Because of the lack of related theoretical work, the range in which ω_{def} is "small enough" remains to be investigated experimentally by performing the proposed NMR–internal-friction experiments. Again, due to the longer-range migration of dislocations, in NMR-fatigue experiments the spin-diffusion limitations of the above theory are much less serious than in internal-friction experiments.

ACKNOWLEDGMENTS

We have benefitted from discussions with Dr. O. Mercier and Dr. D. Paquette. One of us (O.K.) gratefully acknowledges financial support from the Deutsche Forschungsgemeinschaft and the Herbert-Quandt Stiftung.

---

*Present address: Materials Science Division, Argonne National Lab., Argonne, Ill. 60439.

†On leave of absence from the Institut für Physik, Universität Dortmund, V 4600 Dortmund-50, Postfach 500 500, West Germany.

[1]G. Hut, A. W. Sleeswyk, H. J. Hackelöer, H. Selbach, and O. Kanert, Solid State Commun. 15, 1115 (1974).

[2]G. Hut, H. J. Hackelöer, H. Selbach, O. Kanert, and A. W. Sleeswyk, in *Proceedings of the 18th Ampère Congress, Nottingham, 1974* edited by P. S. Allen, E. R. Andrew, and C. A. Bates (Nottingham U. P., Nottingham, 1975), p. 233.

[3]G. Hut, H. J. Hackelöer, H. Selbach, O. Kanert, and A. W. Sleeswyk, Solid State Commun. 17, 85 (1975).

[4]G. Hut, A. W. Sleeswyk, H. J. Hackelöer, H. Selbach, and O. Kanert, Phys. Rev. B 14, 921 (1976).

[5]H. J. Hackelöer, H. Selbach, O. Kanert, A. W. Sleeswyk, and G. Hut, Phys. Status Solidi B 80, 235 (1977).

[6]O. Kanert and M. Mehring, in *NMR, Basic Principles and Progress* edited by P. Diehl, E. Fluck, and R. Kosfeld (Springer, Berlin, 1972), Vol. 3.

[7]A. G. Redfield, Phys. Rev. 98, 1787 (1955).

[8]D. Wolf, Phys. Rev. B 14, 932 (1976).

[9]A. Abragam, *The Principles of Nuclear Magnetism* (Clarendon, Oxford, 1961), Chap. VIII.

[10]Note that these definitions of $V^{(0)}$ and $Q^{(0)}$ deviate, by constant factors, from the usual ones found in the literature. As seen later, this notation has the advantage that corresponding dipolar and quadrupolar expressions for local fields, relaxation rates, etc., may be written in formally identical ways (see also Ref. 11).

[11]D. Wolf, *Spin Temperature and Nuclear Spin Relaxation in Matter: Basic Principles and Applications* (Springer, Berlin, 1977).

[12]T. J. Rowland and F. Y. Fradin, Phys. Rev. 182, 760 (1969).

[13]D. Wolf and P. Jung, Phys. Rev. B 12, 3596 (1975).

[14]C. P. Slichter and D. C. Ailion, Phys. Rev. 135, A1099 (1964).

[15]D. A. McArthur, E. L. Hahn, and R. E. Walstedt, Phys. Rev. 188, 609 (1969).

[16]D. E. Demco, J. Tengenfeldt, and J. S. Waugh, Phys. Rev. B 11, 4133 (1975).

[17]H. C. Torrey, Phys. Rev. 92, 962 (1953).

[18]D. Wolf, Phys. Rev. B 10, 2710 (1974).

[19]D. Wolf, J. Magn. Res. 19, 1 (1975).

[20]A. S. Argon, Philos. Mag. 25, 1053 (1972).

[21]D. Wolf, Phys. Rev. B 15, 37 (1977).

[22]J. J. Gilman, *Micromechanics of Flow in Solids* (McGraw-Hill, New York, 1969), p. 157ff.

[23]J. S. Koehler, in *Imperfections in Nearly Perfect Crystals*, edited by W. Shockley, J. H. Hollomon, R. Maur-

er, and F. Seitz (Wiley, New York, 1952), p. 197ff.
[24]A. V. Granato and K. Lücke, J. Appl. Phys. 27, 583 (1956); and 27, 789 (1956).
[25]R. DeBatist, *Internal Friction of Structural Defects in Crystalline Solids* (North-Holland, Amsterdam, 1972), p. 278ff.
[26]A. Seeger and P. Schiller, *Physical Acoustics* (Academic, New York, 1966), Vol. II.
[27]H. Engelke, Phys. Status Solidi 36, 231 (1969); 36, 245 (1969).
[28]P. R. Moran and P. V. Lang, Phys. Rev. B 2, 2360 (1970).
[29]O. Mercier and D. Paquette (private communication).